

CERN-EP-2020-223
2021/05/26

CMS-SMP-18-003

Measurement of the Z boson differential production cross section using its invisible decay mode ($Z \rightarrow \nu\bar{\nu}$) in proton-proton collisions at $\sqrt{s} = 13$ TeV

The CMS Collaboration*

Abstract

Measurements of the total and differential fiducial cross sections for the Z boson decaying into two neutrinos are presented at the LHC in proton-proton collisions at a center-of-mass energy of 13 TeV. The data were collected by the CMS detector in 2016 and correspond to an integrated luminosity of 35.9 fb^{-1} . In these measurements, events are selected containing an imbalance in transverse momentum and one or more energetic jets. The fiducial differential cross section is measured as a function of the Z boson transverse momentum. The results are combined with a previous measurement of charged-lepton decays of the Z boson. The measured total fiducial cross section for events with Z boson transverse momentum greater than 200 GeV is $3000^{+180}_{-170} \text{ fb}$.

"Published in the Journal of High Energy Physics as doi:10.1007/JHEP05(2021)205."

1 Introduction

The precision measurements of the production of neutrino pairs via the Z boson is an important aspect of the Large Hadron Collider (LHC) program for testing the standard model (SM) of particle physics. They provide a reference for various other measurements in the high energy regime, especially when searching for contributions beyond the SM, where the Z boson production constitutes an important background process. Expectations for the Z boson cross section have been calculated up to next-to-next-to-leading order (NNLO) in perturbative quantum chromodynamics (QCD) and up to next-to-leading order (NLO) in electroweak (EW) production, which correspond to a full NLO EW theory [1–4] supplemented by two-loop Sudakov EW logarithms [5–8]. The calculations are limited by the uncertainties in parton distribution functions (PDFs), and higher-order QCD and EW corrections [9].

Measurements of the differential Z boson production cross sections have been reported by both ATLAS [10–13] and CMS [14–17] at the CERN LHC using charged leptons (electrons or muons) in the final states. In addition, ATLAS has presented differential measurements in pp collisions at $\sqrt{s} = 13$ TeV of the ratio of $Z \rightarrow \nu\nu/Z \rightarrow \ell\ell$ [18] and $ZZ \rightarrow \nu\nu\ell\ell$ production cross sections [19]. In this paper, we present the differential production cross section measurement of Z bosons identified via their decays to pairs of neutrinos. The Z boson branching fraction to neutrinos is about a factor of six times that to electrons or muons, which leads to a smaller statistical uncertainty. This can only be fully exploited at large transverse momenta of the Z boson (p_T^Z), above ≈ 500 GeV, where the measurement of the missing transverse momentum (p_T^{miss}) is sufficiently accurate. This measurement therefore complements those using the charged lepton final states and improves their precision at a higher energy scale. A significant deviation, in particular at large p_T^Z , could reveal signs of physics beyond the SM [20–22].

This paper presents the first inclusive, differential, and normalized fiducial cross section measurements as functions of p_T^Z , where the Z boson is identified via its decay to a pair of neutrinos. The neutrinos are not detected by the CMS detector, but are reconstructed indirectly through the transverse momentum imbalance in the event. We use events with energetic jets and large p_T^{miss} , where the jets mainly arise from the fragmentation and hadronization of quarks or gluons that are produced in the hard scattering process as initial-state radiation. The analysis is based on a data sample of proton-proton (pp) collisions at a center-of-mass energy of 13 TeV, corresponding to an integrated luminosity of $35.9 \pm 0.9 \text{ fb}^{-1}$ collected with the CMS detector at the LHC in 2016.

This paper is organized as follows. A brief overview of the CMS detector is given in Section 2. Information about the definition of objects used in the analysis and the event selection is summarized in Section 3. Event simulations with various Monte Carlo (MC) generators are discussed in Section 4. Section 5 explains the signal-extraction strategy and Section 6 discusses the total, differential, and normalized fiducial cross section measurements. A combined analysis of the current measurements with those from charged leptons is presented in Section 7. Finally, we summarize our results in Section 8. Tabulated results are available in the HepData database [23].

2 The CMS detector and event reconstruction

The central feature of the CMS apparatus is a superconducting solenoid of 6 m internal diameter, providing a magnetic field of 3.8 T. A silicon pixel and strip tracker, a lead tungstate crystal electromagnetic calorimeter (ECAL), and a brass and scintillator hadron calorimeter (HCAL),

each composed of a barrel and two end sections reside within the solenoid volume. Forward calorimeters extend the pseudorapidity (η) coverage provided by the barrel and end-section detectors. Muons are detected in gas-ionization chambers embedded in the steel flux-return yoke outside the solenoid. A more detailed description of the CMS detector, together with a definition of the coordinate system and kinematic variables, can be found in Ref. [24]. Events of interest are selected using a two-tiered trigger system [25]. The first level, composed of custom hardware processors, uses information from the calorimeters and muon detectors at an output rate of ≈ 100 kHz within a fixed latency of about $4 \mu\text{s}$. The second level, known as the high-level trigger, consists of a farm of processors running a version of the full event reconstruction software optimized for fast processing, that reduces the event rate to ≈ 1 kHz before data storage. Additional pp interactions to the studied collision that take place in the same or nearby bunch crossings are referred to as pileup.

Events are reconstructed using a particle-flow (PF) algorithm [26], which combines information from the tracker, calorimeters, and muon systems to reconstruct and identify charged and neutral hadrons, photons, muons, and electrons. The definitions in the following analysis are based on the reconstructed PF candidates, and incorporate additional algorithms and requirements to optimize the selected objects.

Jets are reconstructed by clustering PF candidates using the anti- k_T algorithm [27, 28] with a distance parameter $R = 0.4$. The jet energies are calibrated in the simulation, and separately in data, accounting for energy deposits of neutral particles from pileup and any nonlinear detector response [29, 30]. A charged-hadron subtraction technique, which removes the energy of charged hadrons not originating from the event primary vertex (PV) [31], is applied to mitigate the effect of pileup. The PV is defined as the vertex with the largest value of summed physics-object p_T^2 . Here, the physics objects are the jets clustered using the jet finding algorithm [27, 28] with the tracks assigned to the vertex as inputs, and the associated p_T^{miss} , which is the negative vector p_T sum of those jets. The estimation of p_T^{miss} is improved by propagating the energy correction to the jet four vectors into the sum, as described in Ref. [32].

Jets originating from b quarks are identified (b-tagged) using a multivariate algorithm, referred to as the combined secondary vertex algorithm (CSVv2) [33]. The b tagging working point used in this analysis has a tagging efficiency of $\approx 65\%$ as measured for jets originating from the hadronization of b quarks in top quark pair ($t\bar{t}$) events, with a corresponding mistag rate for jets that originate from the hadronization of light flavor quarks of $\approx 1\%$ [33].

Electron candidates are reconstructed by matching clusters of energy in the ECAL to tracks in the silicon tracker [34]. Clusters compatible with electromagnetic deposition become seeds for electron tracks by back-propagating their trajectories from the calorimeter to the tracker. Tracker seeds are also created from existing tracks by extrapolating their trajectories to the ECAL surface and associating them to PF clusters. After seeds are created, track reconstruction is performed using a dedicated fitting algorithm that includes bremsstrahlung photons that are compatible with originating from an electron track. Additional requirements are applied to reject electrons created in photon conversions in tracker material or jets misreconstructed as electrons. Electron identification criteria rely on observables sensitive to bremsstrahlung along the electron trajectory, the geometrical and momentum-energy matching between the electron trajectory and the associated energy deposit in ECAL, as well as the distribution of energy in the shower and its association with the PV.

Muon candidates are reconstructed in the central tracking system alone or by combining charged tracks in the muon detector with trajectories in the central tracker [35]. Identification criteria based on the number of measurements in the tracker and in the muon system, the fit quality

of the muon track, and its consistency with its origin from the PV are imposed on the muon candidates to reduce the misidentification rate.

Prompt charged leptons are usually isolated, whereas misidentified leptons are often accompanied by charged hadrons or neutral particles. Leptons also arise from a secondary vertex if they are decay products of bottom or charm hadrons. To identify prompt charged leptons we require electrons and muons to satisfy an isolation criterion. An isolation variable is defined by the p_T sum over charged PF candidates associated to the PV and neutral PF particles within a cone around the lepton of radius $\Delta R = \sqrt{(\Delta\eta)^2 + (\Delta\phi)^2} = 0.4$, excluding the lepton. Here $\Delta\phi$ and $\Delta\eta$ refer to the differences in the ϕ (azimuth) and η variables of the PF candidate to the charged-lepton candidate. Isolation cannot be larger than a given maximum value [20]. To mitigate the effect of pileup on this variable, a correction is implemented based on the total event occupancy [36].

Electron and muon candidates must pass certain identification criteria to be selected in the analysis. For the “loose” identification and isolation, they must satisfy $p_T > 10$ GeV and $|\eta| < 2.5$ (2.4) for electrons (muons). At the final stage of the lepton selection, the “tight” working points, following the definitions provided in Ref. [34, 35], are chosen for the identification criteria, including requirements on the impact parameter of the candidates with respect to the PV and their isolation with respect to other particles in the event [37].

The τ leptons that decay to hadrons (τ_h) are identified using the “hadron-plus-strips” algorithm [38]. This algorithm constructs candidates seeded by PF jets that are consistent with τ lepton decay with one or three charged pions. In the single charged pion decay mode, the presence of neutral pions is detected by reconstructing their photonic decays. Mistagged jets originating from non- τ decays are rejected by a discriminator that takes into account the pileup contribution to the neutral component of the τ_h decay [39]. In addition, decay candidates are, in similarity to electron and muon candidates, required to satisfy an isolation criterion as described in Ref. [38].

Photon candidates are reconstructed [40] from clusters in the ECAL that are required to be isolated. The energy deposition in the HCAL tower closest to the seed of the ECAL supercluster [34] assigned to the photon is required to contain $<5\%$ of the energy deposited in the ECAL. The photon isolation is defined by the sum over scalar p_T in a cone centered around the photon momentum vector with a radius of $\Delta R = 0.3$, that excludes the contribution of the photon candidate itself. Corrections for pileup effects are applied to the isolation criteria and depend on the η of the photon.

3 Event selection

We define a signal region (SR) and two control regions (CR). The CRs make use of single-muon and single-lepton events. While the number of signal events is extracted from the SR, the CRs are used to constrain the dominant $W(\ell\nu) + \text{jets}$ background.

3.1 Signal region

For the signal region events are selected using a dedicated triggers designed to select events with large $p_{T, \text{trig}}^{\text{miss}}$ and $H_{T, \text{trig}}^{\text{miss}}$ as calculated with the PF algorithm in the trigger. The observable $p_{T, \text{trig}}^{\text{miss}}$ corresponds to the magnitude of the vector \vec{p}_T sum of all PF candidates reconstructed at the trigger level, while the $H_{T, \text{trig}}^{\text{miss}}$ is the scalar sum of jet p_T s with $p_T > 20$ GeV and $|\eta| < 5.0$ reconstructed at the trigger level. The energy fraction attributed to neutral hadrons in these

jets is required to be smaller than 0.9 to suppress events with jets originating from detector noise. The trigger efficiency is measured to be 97% for events passing the analysis selection with $p_T^{\text{miss}} > 250$ GeV, and becomes 100% for events with $p_T^{\text{miss}} > 350$ GeV [20] with respect to the trigger thresholds of 110 or 120 GeV on $p_{T, \text{trig}}^{\text{miss}}$ and $H_{T, \text{trig}}^{\text{miss}}$ that depend on the data-taking period.

Events are required to have $p_T^{\text{miss}} > 250$ GeV, and the leading jet in the event is required to have $p_T > 100$ GeV and $|\eta| < 2.5$. The leading jet is also required to have at least 10% of its energy associated with charged particles and less than 80% to neutral hadrons. This selection helps to reduce beam-induced background events. In addition, the analysis employs various event filters to reduce large misreconstructed p_T^{miss} backgrounds not originating from beam-beam collisions [32]. The background from $W(\ell\nu) + \text{jets}$ is suppressed by imposing a veto on events containing one or more loosely identified electron or muon with $p_T > 10$ GeV, or τ leptons with $p_T > 18$ GeV. Events that contain an isolated photon with $p_T > 15$ GeV and $|\eta| < 2.5$ are also vetoed to reduce the $\gamma + \text{jets}$ background. To reduce the contamination from top quark backgrounds, events are rejected if they contain an identified b quark jet candidate with $p_T > 20$ GeV and $|\eta| < 2.4$. Finally, production of multijet background events from QCD processes with p_T^{miss} arising from mismeasurements of the jet momenta is suppressed by requiring the minimum azimuthal angle between the \vec{p}_T^{miss} direction and each of the first four jets with p_T greater than 30 GeV ($\Delta\phi(\vec{p}_T^{\text{jet}}, \vec{p}_T^{\text{miss}})$) to be larger than 0.5 radians. The selection requirements in the SR are summarized in Table 1.

Table 1: Summary of the signal region definition.

Variable	Selection	To suppress background from
Electron veto	$p_T > 10$ GeV, $ \eta < 2.5$	$Z \rightarrow \ell\ell + \text{jets}$, $W(\ell\nu) + \text{jets}$
Muon veto	$p_T > 10$ GeV, $ \eta < 2.4$	$Z \rightarrow \ell\ell + \text{jets}$, $W(\ell\nu) + \text{jets}$
τ veto	$p_T > 18$ GeV, $ \eta < 2.3$	$Z \rightarrow \ell\ell + \text{jets}$, $W(\ell\nu) + \text{jets}$
Photon veto	$p_T > 15$ GeV, $ \eta < 2.5$	$\gamma + \text{jets}$
b jet veto	CSVv2 < 0.8484 , $p_T > 20$ GeV, $ \eta < 2.4$	Top quark
p_T^{miss}	> 250 GeV	QCD multijet, top quark, $Z \rightarrow \ell\ell + \text{jets}$
$\Delta\phi(\vec{p}_T^{\text{jet}}, \vec{p}_T^{\text{miss}})$	> 0.5 radians	QCD multijet
Leading jet	$p_T > 100$ GeV, $ \eta < 2.4$	All

3.2 Single-muon control region

The dedicated trigger algorithm discussed for the signal region also provides events for the single-muon CR as the identified PF muons are not considered in the computations of $p_{T, \text{trig}}^{\text{miss}}$ and $H_{T, \text{trig}}^{\text{miss}}$. The single-muon CR is enriched in $W(\mu\nu) + \text{jets}$ events and is defined using the SR criteria with two modifications. First, the muon veto is not applied, and exactly one tightly identified and isolated muon with $p_T > 20$ GeV is required [35]. No additional loosely identified electrons or muons with $p_T > 10$ GeV are accepted. Second, the transverse mass of the muon- \vec{p}_T^{miss} system, given by $m_T = \sqrt{2p_T^{\text{miss}} p_T^\mu (1 - \cos\Delta\phi)}$, where p_T^μ is the p_T of the muon, and $\Delta\phi$ is the azimuthal angle between \vec{p}_T^μ and \vec{p}_T^{miss} , is required to be less than 160 GeV. This suppresses background from QCD multijet events.

3.3 Single-electron control region

The single-electron CR is selected from a different data set based on isolated and non isolated single-electron triggers. The trigger efficiency for the single-electron CR is measured to be $\approx 90\%$ for events passing the selection for electrons with $p_T > 40$ GeV, and becomes fully efficient for events with electron at $p_T > 100$ GeV. The single-electron CR is enriched

in $W(\ell\nu) + \text{jets}$ events and is defined using the trigger selection described above. Events in the single-electron CR are required to contain exactly one tightly identified and isolated electron with $p_T > 40$ GeV [34], and no additional loosely identified electrons or muons with $p_T > 10$ GeV. Finally, the contamination from QCD multijet events is suppressed by requiring $p_T^{\text{miss}} > 50$ GeV and having the m_T of the electron- \vec{p}_T^{miss} system satisfy $m_T < 160$ GeV.

4 Signal and background simulation

Multiple MC event generators are used to simulate the signal and background processes in this analysis. The simulated events are used to optimize selections, evaluate selection efficiencies and systematic uncertainties, and compute expected yields.

Simulated MC samples are produced for the $Z + \text{jets}$ and $W + \text{jets}$ processes at next-to-leading order (NLO) in QCD using the MADGRAPH5_aMC@NLO 2.2.2 [41] generator with up to two additional partons in the matrix element calculations. These events are corrected by vector boson p_T -dependent higher-order EW terms using the multiplicative prescription given in Refs. [1–4, 6, 42].

The QCD multijet processes are generated using MADGRAPH5_aMC@NLO at leading order (LO) in QCD with up to four additional partons in the matrix element calculations. The $t\bar{t}$ and single top quark backgrounds are generated at NLO using POWHEG 2.0 and 1.0, respectively [43–48], and the diboson (WW , WZ , and ZZ) processes are generated at LO in QCD using PYTHIA 8.205 [49].

The MC samples generated using MADGRAPH5_aMC@NLO and POWHEG are interfaced to PYTHIA 8.212 [49] using the CUETP8M1 tune [50] for the fragmentation, hadronization, and underlying event. The MADGRAPH5_aMC@NLO generator provides jets from matrix-element calculations matched to the parton-shower description following the MLM [51] (FxFx [52]) method for LO (and NLO). We use the NNPDF 3.0 [53] PDFs in all generated samples. All MC events are processed through a simulation of the CMS detector based on GEANT4 [54] and are reconstructed with the same algorithms used for data. Additional pileup interactions are also simulated. The distribution of the number of pileup interactions in the simulation is adjusted to match the one observed in the data. The average number of pileup interactions in 2016 was 23.

5 Signal extraction

The largest background contribution in this analysis, about 85%, arises from the $W(\ell\nu) + \text{jets}$ process in events where the charged lepton (electron, muon, or τ -lepton) is either not reconstructed or falls outside the detector acceptance, and is estimated using data from the mutually exclusive CRs selected from single-muon and single-electron final states. The hadronic recoil p_T from the jets is used as an estimator for p_T^{miss} in these control samples, and is defined by excluding any identified electrons or muons from its calculation.

A binned maximum-likelihood fit to the data is performed simultaneously in the SR and the two CRs to estimate the signal and the $W(\ell\nu) + \text{jets}$ background rates in each p_T^{miss} bin. The $W(\ell\nu) + \text{jets}$ background normalization in each p_T^{miss} bin is therefore a free parameter of the fit along with the signal yield:

$$\begin{aligned}
\mathcal{L}(\mu^{W \rightarrow \ell\nu}, \boldsymbol{\mu}, \boldsymbol{\theta}) &= \prod_i \text{Poisson} \left(d_i | B_i(\boldsymbol{\theta}) + \mu_i^{W \rightarrow \ell\nu} + \mu S_i(\boldsymbol{\theta}) \right) \\
&\times \prod_i \text{Poisson} \left(d_i^e | B_i^e(\boldsymbol{\theta}) + \frac{\mu_i^{W \rightarrow \ell\nu}}{R_i^e(\boldsymbol{\theta})} \right) \\
&\times \prod_i \text{Poisson} \left(d_i^\mu | B_i^\mu(\boldsymbol{\theta}) + \frac{\mu_i^{W \rightarrow \ell\nu}}{R_i^\mu(\boldsymbol{\theta})} \right).
\end{aligned}$$

In the above fit, the d_i , d_i^e , and d_i^μ – the symbol i denotes each bin of the p_T^{miss} distribution – are the observed numbers of events in each bin of the SR, single-electron, and single-muon CRs, respectively. The expected contributions from other background processes in the CRs are denoted as B_i^e and B_i^μ . The transfer factors, R_e^W and R_μ^W , are defined as the ratio of the expected yields of the target process in the signal region to the process being measured in the control sample; they are used to constrain the $W(\ell\nu) + \text{jets}$ backgrounds estimated in the SR. The parameter $\mu_i^{W \rightarrow \ell\nu}$ represents the yield of the $W(\ell\nu) + \text{jets}$ background in the i^{th} p_T^{miss} bin, and is left freely floating in the fit. The likelihood also includes a term for the signal region in which B_i represents all the backgrounds apart from $W(\ell\nu) + \text{jets}$, S_i represents the nominal signal prediction, and μ denotes the observed cross section relative to the predicted value. The systematic uncertainties ($\boldsymbol{\theta}$) enter the likelihood as additive perturbations to the transfer factors, and are modeled in the maximum-likelihood fit with Gaussian priors as constrained nuisance parameters that include both experimental and theoretical components.

Both experimental and theoretical uncertainties affecting the transfer factors are included. Experimental uncertainties, including the lepton reconstruction, selection, and veto efficiencies are incorporated into the transfer factors. Lepton veto efficiencies are estimated by propagating them through the uncertainty in the tagging-scale factor to the vetoed selections, whereas the lepton flavor composition of the $W(\ell\nu) + \text{jets}$ process is constrained by the CRs. These experimental uncertainties are only applicable to the leptons in the SR that are not identified, and therefore passed the veto requirement but fall into the detector acceptance. The overall magnitude of the lepton veto uncertainty is determined to be $\approx 2\%$ and is dominated by the τ lepton veto uncertainty. The uncertainties in the efficiency of the electron and p_T^{miss} triggers are also included in the transfer factors. Theoretical uncertainties of the $W(\ell\nu) + \text{jets}$ contributions include the effects from the modeling of uncertainties in the PDFs [55] due to higher-order corrections. All uncertainties discussed are within 1–2% range and are fully correlated across all the bins of hadronic recoil p_T . The full list of uncertainties in the transfer factors are summarized in Table 2.

The remaining backgrounds that contribute to the total event yield in the SR are much smaller than those from $W(\ell\nu) + \text{jets}$. These backgrounds include QCD multijet events, that are measured by extrapolating data from the CR defined by $\Delta\phi(\vec{p}_T^{\text{jet}}, \vec{p}_T^{\text{miss}}) < 0.5$. Top quark, diboson, and $Z \rightarrow \ell\ell + \text{jets}$ (when both leptons are out of acceptance) production are obtained directly from simulation.

Uncertainties assigned to processes estimated from simulation include the uncertainties in the efficiency of the b jet veto, which are estimated to be 3.0 (1.0)% for the top quark (diboson) background. A systematic uncertainty of 10% is included in the top quark background normalization from the modeling of the top quark p_T distribution [56, 57]. Systematic uncertainties of 10 and 20% are included in the normalizations of the top quark [58] and diboson backgrounds [59, 60], respectively, to account for the uncertainties in their cross sections in the

Table 2: Experimental uncertainties affecting transfer factors in the analysis that is used to estimate the $W \rightarrow \ell\nu$ background in the SR. The number of W boson events are denoted as W_{SR} for the SR and in analogy as $W_{\mu\nu}$ ($W_{e\nu}$) for the single-muon (single-electron) CR. The term shape describes the variation in the uncertainty across the hadronic recoil p_{T} or $p_{\text{T}}^{\text{miss}}$ spectra.

Source	Process	Uncertainty (%)
Electron trigger	$W_{\text{SR}}/W_{e\nu}$	1
$p_{\text{T}}^{\text{miss}}$ trigger	$W_{\text{SR}}/W_{e\nu/\mu\nu}$	0–2 (shape)
Muon reconstruction efficiency	$W_{\text{SR}}/W_{\mu\nu}$	1
Muon identification efficiency	$W_{\text{SR}}/W_{\mu\nu}$	1
Electron reconstruction efficiency	$W_{\text{SR}}/W_{e\nu}$	1
Electron identification efficiency	$W_{\text{SR}}/W_{e\nu}$	1.5
Muon veto	$W_{\text{SR}}/W_{e\nu/\mu\nu}$	<1 (shape)
Electron veto	$W_{\text{SR}}/W_{e\nu/\mu\nu}$	<1 (shape)
τ veto	$W_{\text{SR}}/W_{e\nu/\mu\nu}$	1–2 (shape)
PDF	$W_{\text{SR}}/W_{e\nu/\mu\nu}$	1–2 (shape)

relevant kinematic phase space. A systematic uncertainty of 20% is also used to account for the rate of the $Z \rightarrow \ell\ell + \text{jets}$ process, which constitutes less than 0.4% of the total background since this process can only arise in events where the charged lepton is either not reconstructed or falls outside the detector acceptance. The uncertainty in the measurement of the integrated luminosity of 2.5% [61] is assigned to all simulation-based processes. The jet energy scale uncertainties are less than 3% for jets within the tracker acceptance and reach up to 6% for those outside. The uncertainty in the momenta of jets is then propagated to $p_{\text{T}}^{\text{miss}}$ by varying the momenta of each jet within its uncertainty and recomputing $p_{\text{T}}^{\text{miss}}$ [32]. The resulting uncertainty due to jet/ $p_{\text{T}}^{\text{miss}}$ momentum scale is calculated to be 4%. Finally, an uncertainty in the QCD multijet background of 50–150% is assigned to cover differences in the jet response and the statistical uncertainty in the extrapolation from the CR to the SR. These uncertainties are summarized in Table 3.

A cross-check unfolding method was performed, where the background contributions were estimated through a likelihood fit and were subtracted from the data. The alternative unfolding procedure consists of performing a least-squares fit with optional Tikhonov regularization [62], as implemented in the TUnfold software package [63]. The results from this method agree very well with the standard procedure.

6 Fiducial cross section measurements

This analysis provides the Z boson production cross section in a restricted fiducial region and compares with the theoretical predictions. The data selection defined at the reconstruction level is summarized in Table 1. The fiducial phase space, for which theoretical predictions are computed, is defined at the generator level without considering the detector response. The detector resolution leads to a difference between the observables at the reconstruction and the analogous generator level quantities. To minimize discrepancies, the selection criteria imposed at the generator level are defined to mimic the definition at the reconstructed level as much as possible. For this analysis, the fiducial phase space is defined by requiring $p_{\text{T}}^{\text{miss}} > 200 \text{ GeV}$ without any other requirements placed on the Z boson kinematics or the transverse momentum of the leading jet. The $p_{\text{T}}^{\text{miss}}$ is the reconstructed p_{T} of the neutrino pair emitted in Z boson decays.

Table 3: Uncertainties assigned to processes in the SR and CRs. The term shape describes the variation in the uncertainty across the hadronic recoil p_T or p_T^{miss} spectra.

Source	Process	Uncertainty (%)
Luminosity [61]	All	2.5
Electron trigger	All in single-electron CR	1.0
p_T^{miss} trigger	All in SR and single-muon CR	0–2.0 (shape)
Jet/ p_T^{miss} momentum scale	All	4.0
Pileup	All	1.0–2.0 (shape)
Muon reconstruction efficiency	All in single-muon CR	1.0
Muon identification efficiency	All in single-electron CR	1.0
Electron reconstruction efficiency	All in single-electron CR	1.0
Electron identification efficiency	All in single-electron CR	1.5
b jet veto	Top quark in SR and all CRs	3.0
	All remaining in SR and all CRs	1.0
p_T reweighting of top quark	Top quark	10
Top quark normalization	Top quark	10
Normalization of diboson	Diboson	20
$Z \rightarrow \ell\ell + \text{jets}$ normalization	$Z \rightarrow \ell\ell + \text{jets}$ in SR	20
Normalization of QCD multijets	QCD multijets in SR	50–150 (shape)

The difference between fiducial and analysis requirements at the reconstructed level, specifically the requirements on $p_T^{\text{miss}} > 250$ GeV and $p_T^{\text{jet}} > 100$ GeV, introduces a small, $\approx 0.9\%$, theoretical uncertainty from PDFs and missing higher orders in renormalization and factorization scales (QCD scales). These uncertainties are computed by comparing the ratio of theoretical uncertainties in the tighter to the looser analysis phase space requirements. Finally, the contribution arising from events reconstructed within the fiducial phase space, but not originating from there, is treated as background.

To measure the total and differential production cross sections, events in the SR are divided into ten bins of p_T^{miss} , where each bin width is chosen to be at least equal to the p_T^{miss} resolution at the given p_T^{miss} range. A detailed description of the performance of the p_T^{miss} observable is presented in Ref. [32] using $Z + \text{jets}$ and $\gamma + \text{jets}$ events. Based on these p_T^{miss} measurements, the minimum bin width is chosen to be 25 GeV at the lower end of the spectrum and is gradually increased to 350 GeV at the highest p_T^{miss} . The width of the highest p_T^{miss} bin is also chosen to reflect the statistical precision of the sample.

As explained above, to extract the signal and the background, a maximum-likelihood fit is performed using the SR and the CRs. Figure 1 shows the comparison between data and expectations in the SR and CRs before (pre-fit) and after (post-fit) the fit to the data. Pre-fit distributions for the $Z + \text{jets}$ and $W + \text{jets}$ processes are based on simulated MC samples produced at NLO in QCD and are corrected using vector boson p_T -dependent higher-order EW corrections extracted from theoretical calculations. We verified that the measured cross sections are not sensitive to these corrections.

The measured total fiducial cross section is 3000_{-170}^{+180} fb. The corresponding likelihood scan is shown in Fig. 2, together with the predicted value $\sigma_{Z \rightarrow \nu\nu} = 2700 \pm 440$ fb from MADGRAPH5_aMC@NLO using the NNPDF 3.0 [53] NLO PDFs. The theoretical uncertainties for MADGRAPH5_aMC@NLO include statistical, PDF, and QCD-scale uncertainties. The PDF uncertainties are estimated by taking the one standard deviation band of the predictions from the replicas available for samples [64]. The QCD-scale uncertainties are estimated by changing

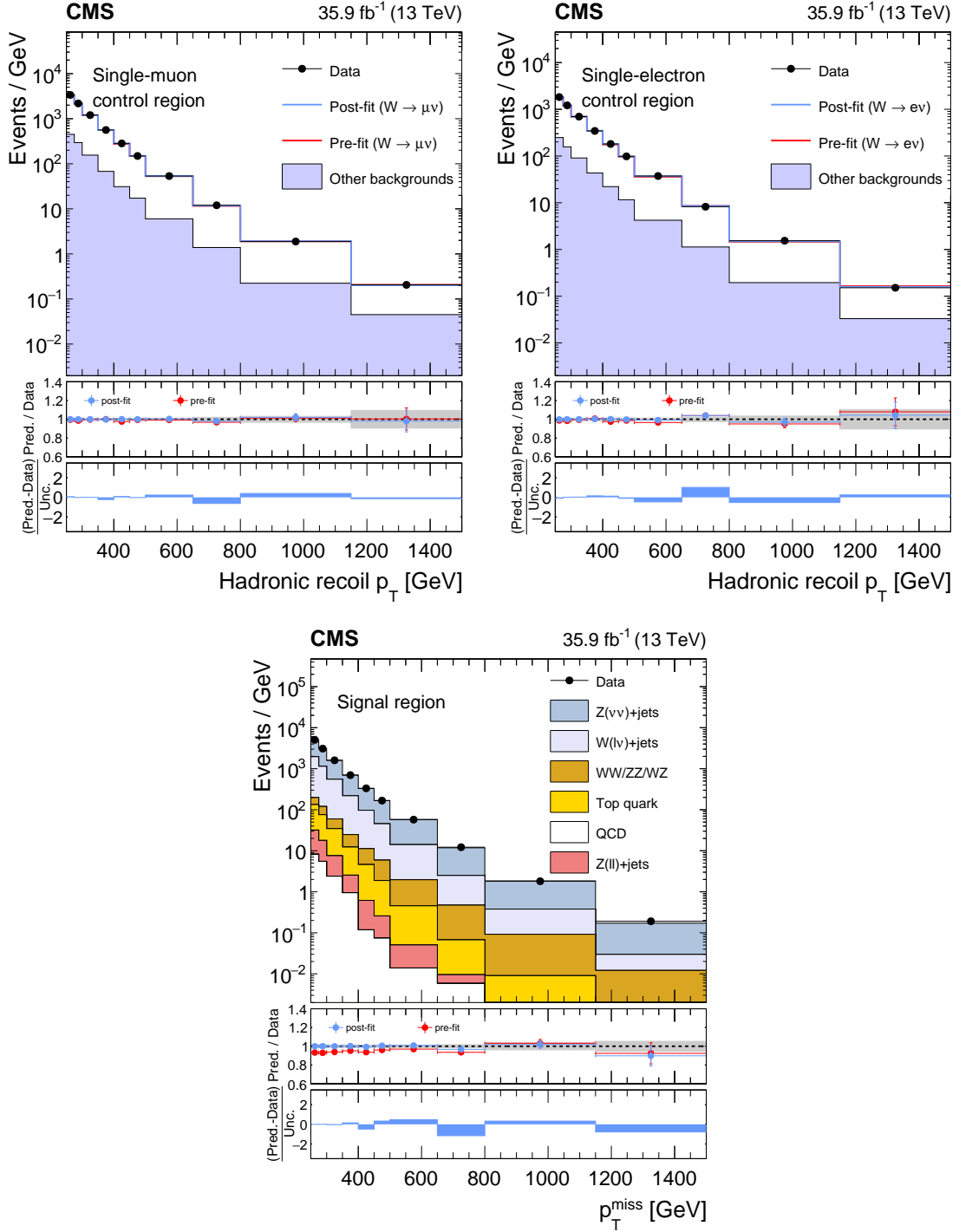


Figure 1: Comparison of data and simulation in the single-muon (upper left), single-electron (upper right) CRs and in the SR (lower), before and after performing the simultaneous fit across all the signal and control regions. The hadronic recoil p_T in single lepton events is used as an estimator for p_T^{miss} in the SR. For the distributions in the CRs, the other backgrounds include top quark, diboson, and QCD multijet events. The post-fit distributions are shown in the upper panel. Ratios of data with the pre-fit expectation (red points) and post-fit prediction (blue points) are shown. The gray band in the ratio panel indicates the post-fit uncertainty after combining all systematic uncertainties. The distribution of the pulls, defined as the difference between data and the post-fit expectation relative to the quadratic sum of the post-fit uncertainties in the expectation, and statistical uncertainty in data, are shown in the lower panel.

the renormalization (μ_R) and factorization (μ_F) scales independently up and down by a factor of two from their nominal values (excluding the two extreme values) and taking the largest changes in the cross section as the uncertainty. The dominant experimental uncertainties are associated with the jet and p_T^{miss} momentum scales and the integrated luminosity.

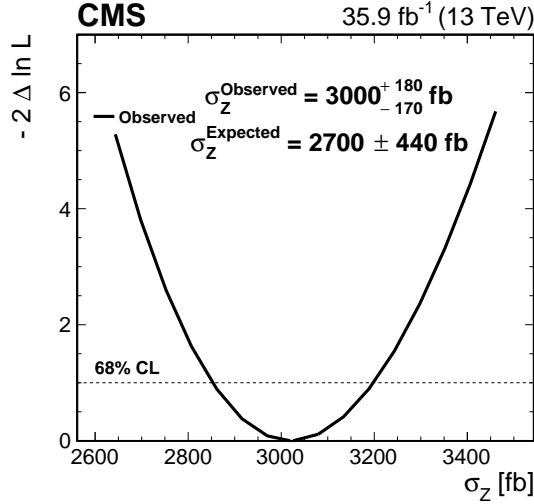


Figure 2: The likelihood scan for the fiducial Z boson production cross section in the $Z \rightarrow \nu\nu$ channel.

In the differential cross section measurement, the signal templates are determined from five differential fiducial regions in p_T^{miss} , and each is allowed to float in the binned fit. The fiducial regions are obtained by combining two neighboring ranges in the reconstructed p_T^{miss} spectra. This stabilizes the fit and ensures that at least 65% of the events in the reconstructed p_T^{miss} bin are also in the same bin in terms of the true p_T of the decaying Z boson. The differential cross section measurements as functions of p_T^Z are shown in Fig. 3 (left) with predictions from MADGRAPH5_aMC@NLO at NLO in QCD and with or without the higher-order EW corrections. These corrections are important at high p_T^Z with expected correction factors of ≈ 0.9 at $p_T^Z = 500$ GeV and ≈ 0.8 at $p_T^Z = 1000$ GeV [9, 65].

The cross section as a function of p_T^Z distribution is also compared to the fixed-order expectation from FEWZ 3.1 [66–69] at NNLO accuracy in QCD ($\mathcal{O}(\alpha_s^2)$, where α_s is the strong coupling) using the NNPDF 3.1 [64] NNLO PDFs. The central values of μ_F and μ_R are chosen to be $\sqrt{q_T^2 + m_Z^2}$, where m_Z is the nominal Z boson mass [70] and q_T is the value of the lower edge of the corresponding bin in p_T^Z . The uncertainties in FEWZ include statistical, PDF, and QCD-scale uncertainties, calculated the same way as for MADGRAPH5_aMC@NLO.

Finally, the data are compared with the NNLO predictions of vector boson production in association with a jet [71] at $\mathcal{O}(\alpha_s^3)$ accuracy using the NNPDF 3.1 [64] NNLO PDFs (referred as NNLOJET in the figures). The central values of μ_F and μ_R are chosen to be $\sqrt{(p_T^Z)^2 + m_{\ell\ell}^2}$. The uncertainties for Z+1 jet at NNLO include PDF and QCD-scales, calculated the same way as for MADGRAPH5_aMC@NLO, and they are largely reduced with respect to other calculations.

Similar to the inclusive measurement, the dominant source of uncertainties are associated with the jet and p_T^{miss} scales and the integrated luminosity. Whereas the systematic uncertainties dominate in the first four fiducial regions, statistical uncertainty dominates in the last signal

bin.

The ratio of the differential cross section relative to the total fiducial cross section (normalized cross section) is also measured using the same binning. In this measurement, the total and individual cross sections are evaluated simultaneously, and therefore, the systematic uncertainties in the individual cross sections are largely reduced. While each fiducial bin is measured separately, only four of these contributions are used to float in the binned maximum-likelihood fit, along with their sum. In this way, the normalized cross section has the same number of degrees of freedom as the differential measurement. The differential cross section measurements normalized to the total cross section are presented in Fig. 3 (right), as well as cross section ratios with respect to the predicted p_T^Z measurements.

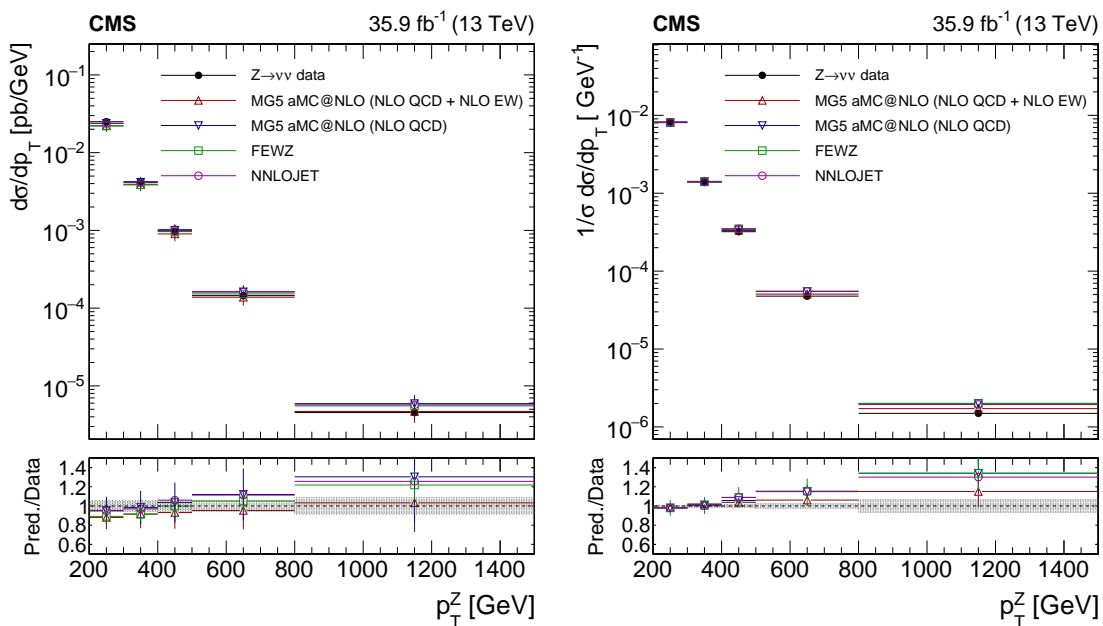


Figure 3: The measured absolute (left) and normalized (right) fiducial cross sections as a function of p_T^Z compared with MADGRAPH5_aMC@NLO and fixed-order calculations. The shaded bands around the data points correspond to the total experimental uncertainty. The vertical bars around the predictions correspond to the combined statistical, PDF, and QCD-scale uncertainties.

7 Combination of cross section measurements using charged leptons and neutrinos

Measurements of differential Z boson production cross section have also been performed with Z bosons decaying to dielectrons or dimuons [17], and these are combined with our new measurements to improve the precision at large p_T^Z . In both analyses, the signal samples are generated with MADGRAPH5_aMC@NLO implemented with the NLO EW corrections applied [9].

While the analysis selection is identical, the fiducial region of the charged-lepton case is modified compared to Ref. [17], to match the definition in Section 6. Specifically, the requirement on the dilepton mass to lie within 15 GeV of the Z boson mass is kept to reduce the photon propagator contribution, but no requirements on the generator-level p_T^ℓ and η^ℓ are applied. The removal of the fiducial requirements on kinematic observables of the leptons is studied in simulation and introduces a small, $\approx 2\%$, theoretical extrapolation uncertainty from PDF and

QCD-scale changes in the $Z \rightarrow \ell\ell$ channel because the reconstruction-level selection requires $p_T^\ell > 25 \text{ GeV}$ and $|\eta^\ell| < 2.4$.

The leading systematic uncertainties between the two analyses are rather different. For the final state with neutrinos, the jet and p_T^{miss} momentum scales uncertainties are dominant, whereas for the charged-lepton final states they originate from lepton identification [17]. Both the jet and p_T^{miss} momentum scales uncertainties and the uncertainties on the lepton identification are kept uncorrelated between the two analyses. The only correlated uncertainty is the integrated luminosity.

The signal cross section is extracted through a simultaneous binned maximum-likelihood fit to the signal and background p_T^{miss} spectra in the SR and CRs of the neutrino channel, as described in Section 6, and to the $p_T^{\ell\ell}$ spectra in the SRs of the charged lepton channel. The individual analyses and the combined differential cross sections are summarized in Table 4.

Table 4: Cross sections (fb) at large p_T^Z values in the $Z \rightarrow \ell\ell$ and $Z \rightarrow \nu\nu$ channels, and their combination. The theoretical predictions from MADGRAPH5_aMC@NLO at NLO in QCD and corrected to NLO in EW [9] using the NNPDF 3.0 are also reported. With the exception of the largest p_T^Z bin, the statistical uncertainties in the measurements are much smaller than the systematic uncertainties. The measurements and predictions correspond to $\sigma\mathcal{B}(Z \rightarrow \ell\ell)$, where σ is the total fiducial cross section, \mathcal{B} is the branching fraction, and ℓ is a charged lepton representing electrons and muons. The $Z \rightarrow \nu\nu$ measurement corresponds to $\sigma\mathcal{B}(Z \rightarrow \ell\ell)/\mathcal{B}(Z \rightarrow \nu\nu)$.

p_T^Z (GeV)	$Z \rightarrow e^+e^-$	$Z \rightarrow \mu^+\mu^-$	$Z \rightarrow \ell\ell$	$Z \rightarrow \nu\nu$	$Z \rightarrow \ell\ell + \nu\nu$	Theory
200–300	2500^{+140}_{-110}	2400^{+120}_{-120}	2500^{+100}_{-100}	2500^{+150}_{-150}	2500^{+82}_{-100}	2200 ± 350
300–400	390^{+22}_{-18}	400^{+22}_{-21}	400^{+17}_{-16}	420^{+24}_{-23}	410^{+14}_{-17}	390 ± 69
400–500	$99^{+5.7}_{-4.9}$	$97^{+6.4}_{-6.1}$	$100^{+4.4}_{-4.2}$	$97^{+5.6}_{-5.4}$	$97^{+3.3}_{-4.0}$	90 ± 18
500–800	$47^{+3.0}_{-2.5}$	$41^{+4.0}_{-3.7}$	$45^{+2.3}_{-2.2}$	$44^{+2.7}_{-2.6}$	$44^{+1.6}_{-1.9}$	41 ± 9.0
800–1500	$3.9^{+0.6}_{-0.5}$	$3.2^{+0.7}_{-0.6}$	$3.7^{+0.4}_{-0.4}$	$3.2^{+0.3}_{-0.3}$	$3.3^{+0.2}_{-0.2}$	3.3 ± 0.9
200–1500	3000^{+160}_{-130}	3000^{+150}_{-140}	3000^{+120}_{-110}	3000^{+180}_{-170}	3000^{+100}_{-120}	2700 ± 440

The combined result leads to a reduction in uncertainties compared with either of the two channels. In the lower- p_T^Z regime, the combination is systematically limited and dominated by the charged-lepton channels. At the same time, at higher p_T^Z , the statistical limitation of the charged-lepton channel is mitigated by the $Z \rightarrow \nu\nu$ channel, yielding improved sensitivity.

The measured experimental distributions are compared with the theoretical predictions from the MADGRAPH5_aMC@NLO generator with and without NLO EW corrections. These distributions are shown in Fig. 4. The uncertainty in the theoretical predictions includes uncertainties both from PDF and from renormalization and factorization scales, together with the statistical precision of the available samples.

The combined cross sections normalized to the total cross section are presented in Fig. 5. Table 5 presents the normalized cross sections relative to the predicted normalized values. The uncertainties due to the jet and p_T^{miss} momentum scales have a smaller p_T^Z distribution dependence than the lepton efficiency uncertainties. Therefore, by evaluating the ratio of cross sections, the uncertainties in the $Z \rightarrow \nu\nu$ channel are more reduced than the ones from the $Z \rightarrow \ell\ell$ channels. While predictions are consistent with data within the experimental and theoretical uncertainties in the full range of p_T^Z , a deviation up to 15% at the highest- p_T^Z regime is observed.

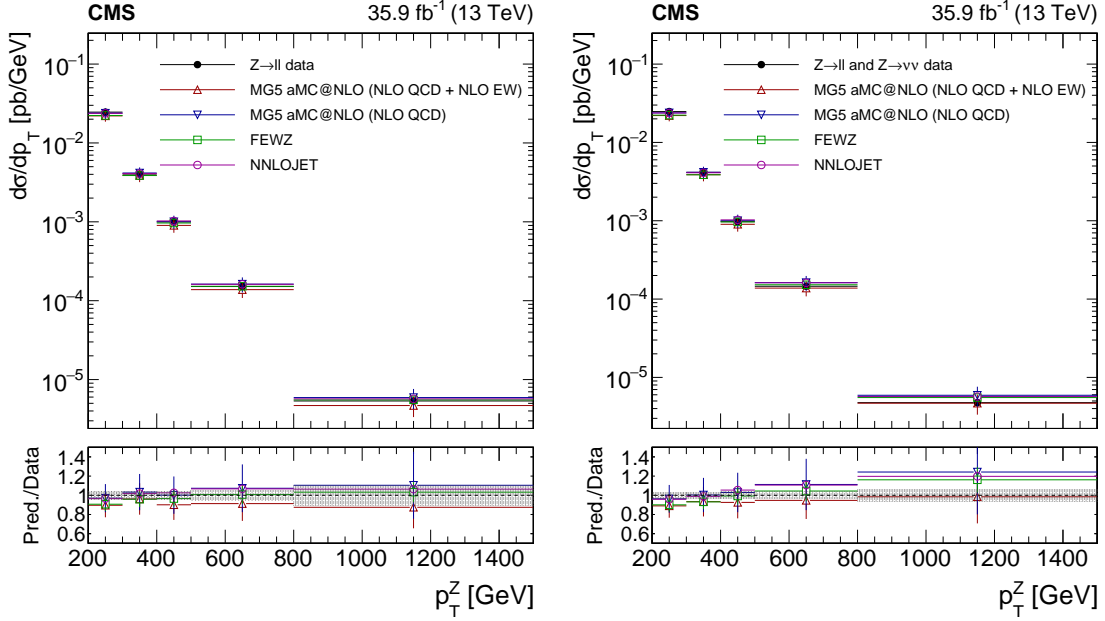


Figure 4: Measured p_T^Z absolute cross section for $Z \rightarrow \ell^+\ell^-$ (left), and the combination (right) being compared with MADGRAPH5_aMC@NLO and fixed-order calculations. The shaded bands around the data points correspond to the total experimental uncertainty. The vertical bars around the predictions correspond to the combined statistical, PDF, and QCD-scale uncertainties.

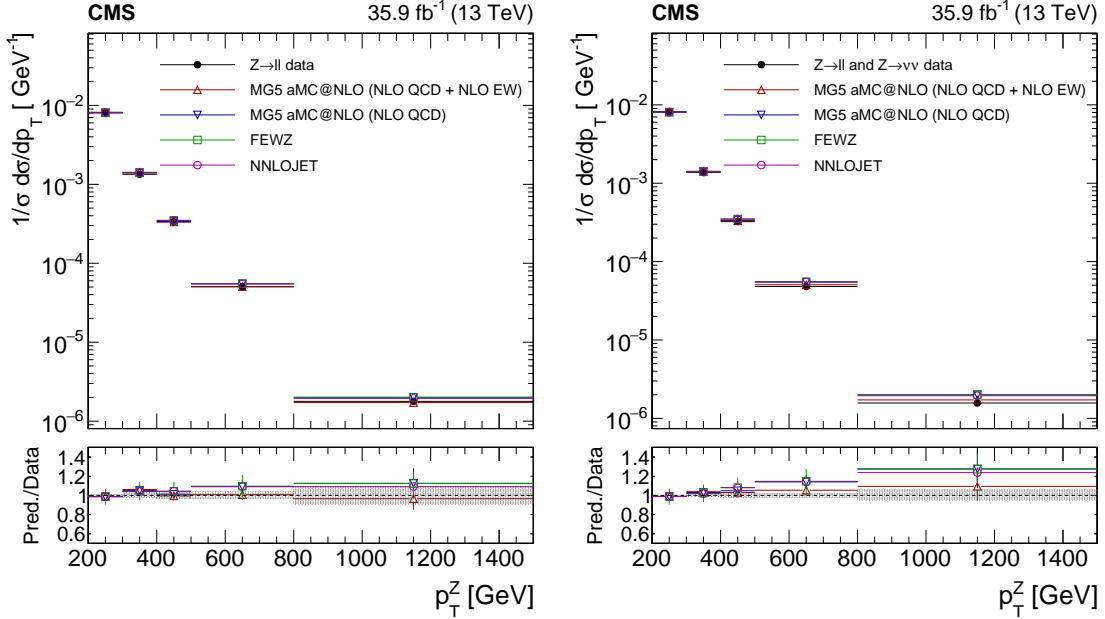


Figure 5: Measured p_T^Z normalized cross section for $Z \rightarrow \ell^+\ell^-$ (left), and the combination (right) compared with MADGRAPH5_aMC@NLO and fixed-order calculations. The shaded bands correspond to the total systematic uncertainty. The vertical bars around the predictions correspond to the combined statistical, PDF, and QCD-scale uncertainties.

Table 5: Cross sections normalized to the total cross section measurements relative to the predicted values in the $Z \rightarrow \ell\ell$ and $Z \rightarrow \nu\nu$ channels, and in their combination. The predicted values are reported in Table 4, and the measured p_T^Z normalized cross sections are shown in Fig. 5.

p_T^Z (GeV)	$Z \rightarrow \ell\ell$	$Z \rightarrow \nu\nu$	$Z \rightarrow \ell\ell + \nu\nu$
200–300	$1.012^{+0.006}_{-0.007}$	$1.019^{+0.009}_{-0.009}$	$1.011^{+0.004}_{-0.004}$
300–400	$0.943^{+0.025}_{-0.025}$	$0.979^{+0.015}_{-0.015}$	$0.963^{+0.015}_{-0.014}$
400–500	$1.006^{+0.031}_{-0.030}$	$0.963^{+0.019}_{-0.019}$	$0.971^{+0.017}_{-0.016}$
500–800	$0.993^{+0.036}_{-0.036}$	$0.942^{+0.024}_{-0.024}$	$0.949^{+0.021}_{-0.020}$
800–1500	$1.036^{+0.099}_{-0.095}$	$0.869^{+0.059}_{-0.057}$	$0.914^{+0.052}_{-0.051}$

8 Summary

Total, differential, and normalized fiducial cross section measurements for a Z boson produced in association with one or more jets in proton-proton collisions at a center-of-mass energy of 13 TeV at high Z boson p_T in the invisible decay channel ($Z \rightarrow \nu\bar{\nu}$) have been presented. The data collected with the CMS detector at the LHC correspond to an integrated luminosity of 35.9 fb^{-1} . The measured total fiducial cross section for events with Z boson transverse momentum greater than 200 GeV is $3000^{+180}_{-170} \text{ fb}$. The precision of this result is improved by combining the cross section measured with those extracted from charged-lepton final states. The results agree within uncertainties with the theoretical predictions from MADGRAPH5_aMC@NLO, FEWZ and Z+1 jet at next-to-next-to-leading order in perturbative quantum chromodynamics. These are the most precise measurements of the p_T^Z spectrum to date in proton-proton collisions at 13 TeV.

Acknowledgments

We congratulate our colleagues in the CERN accelerator departments for the excellent performance of the LHC and thank the technical and administrative staffs at CERN and at other CMS institutes for their contributions to the success of the CMS effort. In addition, we gratefully acknowledge the computing centers and personnel of the Worldwide LHC Computing Grid for delivering so effectively the computing infrastructure essential to our analyses. Finally, we acknowledge the enduring support for the construction and operation of the LHC and the CMS detector provided by the following funding agencies: BMBWF and FWF (Austria); FNRS and FWO (Belgium); CNPq, CAPES, FAPERJ, FAPERGS, and FAPESP (Brazil); MES (Bulgaria); CERN; CAS, MoST, and NSFC (China); COLCIENCIAS (Colombia); MSES and CSF (Croatia); RIF (Cyprus); SENESCYT (Ecuador); MoER, ERC PUT and ERDF (Estonia); Academy of Finland, MEC, and HIP (Finland); CEA and CNRS/IN2P3 (France); BMBF, DFG, and HGF (Germany); GSRT (Greece); NKFI (Hungary); DAE and DST (India); IPM (Iran); SFI (Ireland); INFN (Italy); MSIP and NRF (Republic of Korea); MES (Latvia); LAS (Lithuania); MOE and UM (Malaysia); BUAP, CINVESTAV, CONACYT, LNS, SEP, and UASLP-FAI (Mexico); MOS (Montenegro); MBIE (New Zealand); PAEC (Pakistan); MSHE and NSC (Poland); FCT (Portugal); JINR (Dubna); MON, RosAtom, RAS, RFBR, and NRC KI (Russia); MESTD (Serbia); SEIDI, CPAN, PCTI, and FEDER (Spain); MOSTR (Sri Lanka); Swiss Funding Agencies (Switzerland); MST (Taipei); ThEPCenter, IPST, STAR, and NSTDA (Thailand); TUBITAK and TAEK (Turkey); NASU (Ukraine); STFC (United Kingdom); DOE and NSF (USA).

Individuals have received support from the Marie-Curie program and the European Research Council and Horizon 2020 Grant, contract Nos. 675440, 724704, 752730, and 765710 (European Union); the Leventis Foundation; the A.P. Sloan Foundation; the Alexander von Humboldt Foundation; the Belgian Federal Science Policy Office; the Fonds pour la Formation à la Recherche dans l'Industrie et dans l'Agriculture (FRIA-Belgium); the Agentschap voor Innovatie door Wetenschap en Technologie (IWT-Belgium); the F.R.S.-FNRS and FWO (Belgium) under the "Excellence of Science – EOS" – be.h project n. 30820817; the Beijing Municipal Science & Technology Commission, No. Z191100007219010; the Ministry of Education, Youth and Sports (MEYS) of the Czech Republic; the Deutsche Forschungsgemeinschaft (DFG) under Germany's Excellence Strategy – EXC 2121 "Quantum Universe" – 390833306; the Lendület ("Momentum") Program and the János Bolyai Research Scholarship of the Hungarian Academy of Sciences, the New National Excellence Program ÚNKP, the NKFI research grants 123842, 123959, 124845, 124850, 125105, 128713, 128786, and 129058 (Hungary); the Council of Science and Industrial Research, India; the HOMING PLUS program of the Foundation for Polish Science, cofinanced from European Union, Regional Development Fund, the Mobility Plus program of the Ministry of Science and Higher Education, the National Science Center (Poland), contracts Harmonia 2014/14/M/ST2/00428, Opus 2014/13/B/ST2/02543, 2014/15/B/ST2/03998, and 2015/19/B/ST2/02861, Sonata-bis 2012/07/E/ST2/01406; the National Priorities Research Program by Qatar National Research Fund; the Ministry of Science and Higher Education, project no. 0723-2020-0041 (Russia); the Tomsk Polytechnic University Competitiveness Enhancement Program; the Programa Estatal de Fomento de la Investigación Científica y Técnica de Excelencia María de Maeztu, grant MDM-2015-0509 and the Programa Severo Ochoa del Principado de Asturias; the Thalís and Aristeia programs cofinanced by EU-ESF and the Greek NSRF; the Rachadapisek Sompot Fund for Postdoctoral Fellowship, Chulalongkorn University and the Chulalongkorn Academic into Its 2nd Century Project Advancement Project (Thailand); the Kavli Foundation; the Nvidia Corporation; the SuperMicro Corporation; the Welch Foundation, contract C-1845; and the Weston Havens Foundation (USA).

References

- [1] A. Denner, S. Dittmaier, T. Kasprzik, and A. Muck, "Electroweak corrections to $W + \text{jet}$ hadroproduction including leptonic W -boson decays", *JHEP* **08** (2009) 075, doi:10.1088/1126-6708/2009/08/075, arXiv:0906.1656.
- [2] A. Denner, S. Dittmaier, T. Kasprzik, and A. Muck, "Electroweak corrections to dilepton + jet production at hadron colliders", *JHEP* **06** (2011) 069, doi:10.1007/JHEP06(2011)069, arXiv:1103.0914.
- [3] A. Denner, S. Dittmaier, T. Kasprzik, and A. Mack, "Electroweak corrections to monojet production at the LHC", *Eur. Phys. J. C* **73** (2013) 2297, doi:10.1140/epjc/s10052-013-2297-x, arXiv:1211.5078.
- [4] S. Kallweit et al., "NLO QCD+EW predictions for $V + \text{jets}$ including off-shell vector-boson decays and multijet merging", *JHEP* **04** (2016) 021, doi:10.1007/JHEP04(2016)021, arXiv:1511.08692.
- [5] J. H. Kuhn, A. Kulesza, S. Pozzorini, and M. Schulze, "Logarithmic electroweak corrections to hadronic $Z+1$ jet production at large transverse momentum", *Phys. Lett. B* **609** (2005) 277, doi:10.1016/j.physletb.2005.01.059, arXiv:hep-ph/0408308.

-
- [6] J. H. Kuhn, A. Kulesza, S. Pozzorini, and M. Schulze, “Electroweak corrections to hadronic photon production at large transverse momenta”, *JHEP* **03** (2006) 059, doi:10.1088/1126-6708/2006/03/059, arXiv:hep-ph/0508253.
- [7] J. H. Kuhn, A. Kulesza, S. Pozzorini, and M. Schulze, “One-loop weak corrections to hadronic production of Z bosons at large transverse momenta”, *Nucl. Phys. B* **727** (2005) 368, doi:10.1016/j.nuclphysb.2005.08.019, arXiv:hep-ph/0507178.
- [8] J. H. Kuhn, A. Kulesza, S. Pozzorini, and M. Schulze, “Electroweak corrections to hadronic production of W bosons at large transverse momenta”, *Nucl. Phys. B* **797** (2008) 27, doi:10.1016/j.nuclphysb.2007.12.029, arXiv:0708.0476.
- [9] J. M. Lindert et al., “Precise predictions for V+jets dark matter backgrounds”, *Eur. Phys. J. C* **77** (2017) 829, doi:10.1140/epjc/s10052-017-5389-1, arXiv:1705.04664.
- [10] ATLAS Collaboration, “Measurement of the transverse momentum distribution of Z/ γ^* bosons in proton-proton collisions at $\sqrt{s} = 7$ TeV with the ATLAS detector”, *Phys. Lett. B* **705** (2011) 415, doi:10.1016/j.physletb.2011.10.018, arXiv:1107.2381.
- [11] ATLAS Collaboration, “Measurement of the Z/ γ^* boson transverse momentum distribution in pp collisions at $\sqrt{s} = 7$ TeV with the ATLAS detector”, *JHEP* **09** (2014) 145, doi:10.1007/JHEP09(2014)145, arXiv:1406.3660.
- [12] ATLAS Collaboration, “Measurement of the transverse momentum and ϕ_{η}^* distributions of Drell-Yan lepton pairs in proton-proton collisions at $\sqrt{s} = 8$ TeV with the ATLAS detector”, *Eur. Phys. J. C* **76** (2016) 291, doi:10.1140/epjc/s10052-016-4070-4, arXiv:1512.02192.
- [13] ATLAS Collaboration, “Measurement of the transverse momentum distribution of Drell-Yan lepton pairs in proton-proton collisions at $\sqrt{s} = 13$ TeV with the ATLAS detector”, *Eur. Phys. J. C* **80** (2020) 616, doi:10.1140/epjc/s10052-020-8001-z, arXiv:1912.02844.
- [14] CMS Collaboration, “Measurement of the rapidity and transverse momentum distributions of Z bosons in pp collisions at $\sqrt{s} = 7$ TeV”, *Phys. Rev. D* **85** (2012) 032002, doi:10.1103/PhysRevD.85.032002, arXiv:1110.4973.
- [15] CMS Collaboration, “Measurement of the Z boson differential cross section in transverse momentum and rapidity in proton-proton collisions at 8 TeV”, *Phys. Lett. B* **749** (2015) 187, doi:10.1016/j.physletb.2015.07.065, arXiv:1504.03511.
- [16] CMS Collaboration, “Measurements of differential and double-differential Drell-Yan cross sections in proton-proton collisions at $\sqrt{s} = 8$ TeV”, *Eur. Phys. J. C* **75** (2015) 147, doi:10.1140/epjc/s10052-015-3364-2, arXiv:1412.1115.
- [17] CMS Collaboration, “Measurements of differential Z boson production cross sections in proton-proton collisions at $\sqrt{s} = 13$ TeV”, *JHEP* **12** (2019) 061, doi:10.1007/JHEP12(2019)061, arXiv:1909.04133.
- [18] ATLAS Collaboration, “Measurement of detector-corrected observables sensitive to the anomalous production of events with jets and large missing transverse momentum in pp collisions at $\sqrt{s} = 13$ TeV using the ATLAS detector”, *Eur. Phys. J. C* **77** (2017), no. 11, 765, doi:10.1140/epjc/s10052-017-5315-6, arXiv:1707.03263.

- [19] ATLAS Collaboration, “Measurement of ZZ production in the $\ell\ell\nu\nu$ final state with the ATLAS detector in pp collisions at $\sqrt{s} = 13$ TeV”, *JHEP* **10** (2019) 127, doi:10.1007/JHEP10(2019)127, arXiv:1905.07163.
- [20] CMS Collaboration, “Search for new physics in final states with an energetic jet or a hadronically decaying W or Z boson and transverse momentum imbalance at $\sqrt{s} = 13$ TeV”, *Phys. Rev. D* **97** (2018) 092005, doi:10.1103/PhysRevD.97.092005, arXiv:1712.02345.
- [21] CMS Collaboration, “Search for invisible decays of a Higgs boson produced through vector boson fusion in proton-proton collisions at $\sqrt{s} = 13$ TeV”, *Phys. Lett. B* **793** (2019) 520, doi:10.1016/j.physletb.2019.04.025, arXiv:1809.05937.
- [22] CMS Collaboration, “Search for supersymmetry in proton-proton collisions at 13 TeV in final states with jets and missing transverse momentum”, *JHEP* **10** (2019) 244, doi:10.1007/JHEP10(2019)244, arXiv:1908.04722.
- [23] “HEPData record for this analysis”. doi:10.17182/hepdata.96028.
- [24] CMS Collaboration, “The CMS experiment at the CERN LHC”, *JINST* **3** (2008) S08004, doi:10.1088/1748-0221/3/08/S08004.
- [25] CMS Collaboration, “The CMS trigger system”, *JINST* **12** (2017) P01020, doi:10.1088/1748-0221/12/01/P01020, arXiv:1609.02366.
- [26] CMS Collaboration, “Particle-flow reconstruction and global event description with the CMS detector”, *JINST* **12** (2017) P10003, doi:10.1088/1748-0221/12/10/P10003, arXiv:1706.04965.
- [27] M. Cacciari and G. P. Salam and G. Soyez, “The anti- k_T jet clustering algorithm”, *JHEP* **04** (2008) 063, doi:10.1088/1126-6708/2008/04/063, arXiv:0802.1189.
- [28] M. Cacciari, G. P. Salam, and G. Soyez, “FastJet user manual”, *Eur. Phys. J. C* **72** (2012) 1896, doi:10.1140/epjc/s10052-012-1896-2, arXiv:1111.6097.
- [29] CMS Collaboration, “Jet energy scale and resolution in the CMS experiment in pp collisions at 8 TeV”, *JINST* **12** (2017) P02014, doi:10.1088/1748-0221/12/02/P02014, arXiv:1607.03663.
- [30] CMS Collaboration, “Jet energy scale and resolution performance with 13 TeV data collected by CMS in 2016-2018”, CMS Detector Performance Summary CMS-DP-2020-019, 2020.
- [31] CMS Collaboration, “Pileup mitigation at CMS in 13 TeV data”, *JINST* **15** (2020) P09018, doi:10.1088/1748-0221/15/09/P09018, arXiv:2003.00503.
- [32] CMS Collaboration, “Performance of missing transverse momentum reconstruction in proton-proton collisions at $\sqrt{s} = 13$ TeV using the CMS detector”, *JINST* **14** (2019) P07004, doi:10.1088/1748-0221/14/07/P07004, arXiv:1903.06078.
- [33] CMS Collaboration, “Identification of heavy-flavour jets with the CMS detector in pp collisions at 13 TeV”, *JINST* **13** (2018) P05011, doi:10.1088/1748-0221/13/05/P05011, arXiv:1712.07158.

-
- [34] CMS Collaboration, “Performance of electron reconstruction and selection with the CMS detector in proton-proton collisions at $\sqrt{s} = 8$ TeV”, *JINST* **10** (2015) P06005, doi:10.1088/1748-0221/10/06/P06005, arXiv:1502.02701.
- [35] CMS Collaboration, “Performance of the CMS muon detector and muon reconstruction with proton-proton collisions at $\sqrt{s} = 13$ TeV”, *JINST* **13** (2018) P06015, doi:10.1088/1748-0221/13/06/P06015, arXiv:1804.04528.
- [36] M. Cacciari and G. P. Salam, “Pileup subtraction using jet areas”, *Phys. Lett. B* **659** (2008) 119, doi:10.1016/j.physletb.2007.09.077, arXiv:0707.1378.
- [37] CMS Collaboration, “Measurements of properties of the Higgs boson decaying to a W boson pair in pp collisions at $\sqrt{s} = 13$ TeV”, *Phys. Lett. B* **791** (2019) 96, doi:10.1016/j.physletb.2018.12.073, arXiv:1806.05246.
- [38] CMS Collaboration, “Reconstruction and identification of τ lepton decays to hadrons and ν_τ at CMS”, *JINST* **11** (2016) P01019, doi:10.1088/1748-0221/11/01/P01019, arXiv:1510.07488.
- [39] CMS Collaboration, “Performance of reconstruction and identification of τ leptons decaying to hadrons and ν_τ in pp collisions at $\sqrt{s} = 13$ TeV”, *JINST* **13** (2018) P10005, doi:10.1088/1748-0221/13/10/P10005, arXiv:1809.02816.
- [40] CMS Collaboration, “Performance of photon reconstruction and identification with the CMS detector in proton-proton collisions at $\sqrt{s} = 8$ TeV”, *JINST* **10** (2015) P08010, doi:10.1088/1748-0221/10/08/P08010, arXiv:1502.02702.
- [41] J. Alwall et al., “The automated computation of tree-level and next-to-leading order differential cross sections, and their matching to parton shower simulations”, *JHEP* **07** (2014) 079, doi:10.1007/JHEP07(2014)079, arXiv:1405.0301.
- [42] S. Kallweit et al., “NLO electroweak automation and precise predictions for W+multijet production at the LHC”, *JHEP* **04** (2015) 012, doi:10.1007/JHEP04(2015)012, arXiv:1412.5157.
- [43] P. Nason, “A new method for combining NLO QCD with shower Monte Carlo algorithms”, *JHEP* **11** (2004) 040, doi:10.1088/1126-6708/2004/11/040, arXiv:hep-ph/0409146.
- [44] S. Frixione, P. Nason, and C. Oleari, “Matching NLO QCD computations with parton shower simulations: the POWHEG method”, *JHEP* **11** (2007) 070, doi:10.1088/1126-6708/2007/11/070, arXiv:0709.2092.
- [45] S. Alioli, P. Nason, C. Oleari, and E. Re, “A general framework for implementing NLO calculations in shower Monte Carlo programs: the POWHEG BOX”, *JHEP* **06** (2010) 043, doi:10.1007/JHEP06(2010)043, arXiv:1002.2581.
- [46] P. Nason and G. Zanderighi, “ W^+W^- , WZ and ZZ production in the POWHEG-BOX-V2”, *Eur. Phys. J. C* **74** (2014) 2702, doi:10.1140/epjc/s10052-013-2702-5, arXiv:1311.1365.
- [47] S. Alioli, P. Nason, C. Oleari, and E. Re, “NLO vector-boson production matched with shower in POWHEG”, *JHEP* **07** (2008) 060, doi:10.1088/1126-6708/2008/07/060, arXiv:0805.4802.

- [48] S. Alioli, P. Nason, C. Oleari, and E. Re, “NLO Higgs boson production via gluon fusion matched with shower in POWHEG”, *JHEP* **04** (2009) 002, doi:10.1088/1126-6708/2009/04/002, arXiv:0812.0578.
- [49] T. Sjöstrand et al., “An introduction to PYTHIA 8.2”, *Comput. Phys. Commun.* **191** (2015) 159, doi:10.1016/j.cpc.2015.01.024, arXiv:1410.3012.
- [50] CMS Collaboration, “Event generator tunes obtained from underlying event and multiparton scattering measurements”, *Eur. Phys. J. C* **76** (2016) 155, doi:10.1140/epjc/s10052-016-3988-x, arXiv:1512.00815.
- [51] M. L. Mangano, M. Moretti, F. Piccinini, and M. Treccani, “Matching matrix elements and shower evolution for top-quark production in hadronic collisions”, *JHEP* **01** (2007) 013, doi:10.1088/1126-6708/2007/01/013, arXiv:hep-ph/0611129.
- [52] R. Frederix and S. Frixione, “Merging meets matching in MC@NLO”, *JHEP* **12** (2012) 061, doi:10.1007/JHEP12(2012)061, arXiv:1209.6215.
- [53] NNPDF Collaboration, “Parton distributions for the LHC Run II”, *JHEP* **04** (2015) 040, doi:10.1007/JHEP04(2015)040, arXiv:1410.8849.
- [54] GEANT4 Collaboration, “GEANT4 — a simulation toolkit”, *Nucl. Instrum. Meth. A* **506** (2003) 250, doi:10.1016/S0168-9002(03)01368-8.
- [55] J. Butterworth et al., “PDF4LHC recommendations for LHC Run II”, *J. Phys. G* **43** (2016) 023001, doi:10.1088/0954-3899/43/2/023001, arXiv:1510.03865.
- [56] M. Czakon et al., “Top-pair production at the LHC through NNLO QCD and NLO EW”, *JHEP* **10** (2017) 186, doi:10.1007/JHEP10(2017)186, arXiv:1705.04105.
- [57] CMS Collaboration, “Measurement of differential cross sections for top quark pair production using the lepton+jets final state in proton-proton collisions at 13 TeV”, *Phys. Rev. D* **95** (2017) 092001, doi:10.1103/PhysRevD.95.092001, arXiv:1610.04191.
- [58] CMS Collaboration, “Measurement of the top quark pair production cross section in proton-proton collisions at $\sqrt{s} = 13$ TeV”, *Phys. Rev. Lett.* **116** (2016) 052002, doi:10.1103/PhysRevLett.116.052002, arXiv:1510.05302.
- [59] CMS Collaboration, “Measurement of the ZZ production cross section and $Z \rightarrow \ell^+ \ell^- \ell'^+ \ell'^-$ branching fraction in pp collisions at $\sqrt{s} = 13$ TeV”, *Phys. Lett. B* **763** (2016) 280, doi:10.1016/j.physletb.2016.10.054, arXiv:1607.08834.
- [60] CMS Collaboration, “Measurement of the WZ production cross section in pp collisions at $\sqrt{s} = 13$ TeV”, *Phys. Lett. B* **766** (2017) 268, doi:10.1016/j.physletb.2017.01.011, arXiv:1607.06943.
- [61] CMS Collaboration, “CMS luminosity measurement for the 2016 data-taking period”, CMS Physics Analysis Summary CMS-PAS-LUM-17-001, 2017.
- [62] I. V. Tikhonov, “Solution of incorrectly formulated problems and the regularization method”, *Soviet Mathematics* **4** (1963) 1023.
- [63] S. Schmitt, “TUnfold: an algorithm for correcting migration effects in high energy physics”, *JINST* **7** (2012) T10003, doi:10.1088/1748-0221/7/10/T10003, arXiv:1205.6201.

- [64] NNPDF Collaboration, “Parton distributions from high-precision collider data”, *Eur. Phys. J. C* **77** (2017) 663, doi:10.1140/epjc/s10052-017-5199-5, arXiv:1706.00428.
- [65] S. Dittmaier, A. Huss, and C. Schwinn, “Mixed QCD-electroweak $\mathcal{O}(\alpha_s\alpha)$ corrections to Drell-Yan processes in the resonance region: pole approximation and non-factorizable corrections”, *Nucl. Phys. B* **885** (2014) 318, doi:10.1016/j.nuclphysb.2014.05.027, arXiv:1403.3216.
- [66] K. Melnikov and F. Petriello, “The W boson production cross section at the LHC through $\mathcal{O}(\alpha_s^2)$ ”, *Phys. Rev. Lett.* **96** (2006) 231803, doi:10.1103/PhysRevLett.96.231803, arXiv:hep-ph/0603182.
- [67] R. Gavin, Y. Li, F. Petriello, and S. Quackenbush, “FEWZ 2.0: A code for hadronic Z production at next-to-next-to-leading order”, *Comput. Phys. Commun.* **182** (2011) 2388, doi:10.1016/j.cpc.2011.06.008, arXiv:1011.3540.
- [68] R. Gavin, Y. Li, F. Petriello, and S. Quackenbush, “W physics at the LHC with FEWZ 2.1”, *Comput. Phys. Commun.* **184** (2013) 208, doi:10.1016/j.cpc.2012.09.005, arXiv:1201.5896.
- [69] Y. Li and F. Petriello, “Combining QCD and electroweak corrections to dilepton production in FEWZ”, *Phys. Rev. B* **86** (2012) 094034, doi:10.1103/PhysRevD.86.094034, arXiv:1208.5967.
- [70] Particle Data Group, P. A. Zyla et al., “Review of particle physics”, *Prog. Theor. Exp. Phys.* **2020** (2020) 083C01, doi:10.1093/ptep/ptaa104.
- [71] A. Gehrmann-De Ridder et al., “Precise QCD predictions for the production of a Z boson in association with a hadronic jet”, *Phys. Rev. Lett.* **117** (2016) 022001, doi:10.1103/PhysRevLett.117.022001, arXiv:1507.02850.

A The CMS Collaboration

Yerevan Physics Institute, Yerevan, Armenia

A.M. Sirunyan[†], A. Tumasyan

Institut für Hochenergiephysik, Wien, Austria

W. Adam, T. Bergauer, M. Dragicevic, A. Escalante Del Valle, R. Frühwirth¹, M. Jeitler¹, N. Krammer, L. Lechner, D. Liko, I. Mikulec, F.M. Pitters, J. Schieck¹, R. Schöfbeck, M. Spanring, S. Templ, W. Waltenberger, C.-E. Wulz¹, M. Zarucki

Institute for Nuclear Problems, Minsk, Belarus

V. Chekhovsky, A. Litomin, V. Makarenko

Universiteit Antwerpen, Antwerpen, Belgium

M.R. Darwish², E.A. De Wolf, X. Janssen, T. Kello³, A. Lelek, M. Pieters, H. Rejeb Sfar, P. Van Mechelen, S. Van Putte, N. Van Remortel

Vrije Universiteit Brussel, Brussel, Belgium

F. Blekman, E.S. Bols, J. D'Hondt, J. De Clercq, D. Lontkovskyi, S. Lowette, I. Marchesini, S. Moortgat, A. Morton, D. Müller, A.R. Sahasransu, S. Tavernier, W. Van Doninck, P. Van Mulders

Université Libre de Bruxelles, Bruxelles, Belgium

D. Beghin, B. Bilin, B. Clerbaux, G. De Lentdecker, B. Dorney, L. Favart, A. Grebenyuk, A.K. Kalsi, K. Lee, I. Makarenko, L. Moureaux, L. Pétré, A. Popov, N. Postiau, E. Starling, L. Thomas, C. Vander Velde, P. Vanlaer, D. Vannerom, L. Wezenbeek

Ghent University, Ghent, Belgium

T. Cornelis, D. Dobur, M. Gruchala, I. Khvastunov⁴, G. Mestdach, M. Niedziela, C. Roskas, K. Skovpen, M. Tytgat, W. Verbeke, B. Vermassen, M. Vit

Université Catholique de Louvain, Louvain-la-Neuve, Belgium

A. Bethani, G. Bruno, F. Bury, C. Caputo, P. David, C. Delaere, M. Delcourt, I.S. Donertas, A. Giammanco, V. Lemaitre, K. Mondal, J. Prisciandaro, A. Taliencio, M. Teklishyn, P. Vischia, S. Wertz, S. Wuyckens

Centro Brasileiro de Pesquisas Fisicas, Rio de Janeiro, Brazil

G.A. Alves, C. Hensel, A. Moraes

Universidade do Estado do Rio de Janeiro, Rio de Janeiro, Brazil

W.L. Aldá Júnior, E. Belchior Batista Das Chagas, H. BRANDAO MALBOUISSON, W. Carvalho, J. Chinellato⁵, E. Coelho, E.M. Da Costa, G.G. Da Silveira⁶, D. De Jesus Damiao, S. Fonseca De Souza, J. Martins⁷, D. Matos Figueiredo, C. Mora Herrera, L. Mundim, H. Nogima, P. Rebello Teles, L.J. Sanchez Rosas, A. Santoro, S.M. Silva Do Amaral, A. Sznajder, M. Thiel, F. Torres Da Silva De Araujo, A. Vilela Pereira

Universidade Estadual Paulista ^a, Universidade Federal do ABC ^b, São Paulo, Brazil

C.A. Bernardes^{a,a}, L. Calligaris^a, T.R. Fernandez Perez Tomei^a, E.M. Gregores^{a,b}, D.S. Lemos^a, P.G. Mercadante^{a,b}, S.F. Novaes^a, Sandra S. Padula^a

Institute for Nuclear Research and Nuclear Energy, Bulgarian Academy of Sciences, Sofia, Bulgaria

A. Aleksandrov, G. Antchev, I. Atanasov, R. Hadjiiska, P. Iaydjiev, M. Misheva, M. Rodozov, M. Shopova, G. Sultanov

University of Sofia, Sofia, Bulgaria

A. Dimitrov, T. Ivanov, L. Litov, B. Pavlov, P. Petkov, A. Petrov

Beihang University, Beijing, China

T. Cheng, W. Fang³, Q. Guo, M. Mittal, H. Wang, L. Yuan

Department of Physics, Tsinghua University, Beijing, China

M. Ahmad, G. Bauer, Z. Hu, Y. Wang, K. Yi^{8,9}

Institute of High Energy Physics, Beijing, China

E. Chapon, G.M. Chen¹⁰, H.S. Chen¹⁰, M. Chen, T. Javaid¹⁰, A. Kapoor, D. Leggat, H. Liao, Z.-A. LIU¹⁰, R. Sharma, A. Spiezia, J. Tao, J. Thomas-wilsker, J. Wang, H. Zhang, S. Zhang¹⁰, J. Zhao

State Key Laboratory of Nuclear Physics and Technology, Peking University, Beijing, China

A. Agapitos, Y. Ban, C. Chen, Q. Huang, A. Levin, Q. Li, M. Lu, X. Lyu, Y. Mao, S.J. Qian, D. Wang, Q. Wang, J. Xiao

Sun Yat-Sen University, Guangzhou, China

Z. You

Institute of Modern Physics and Key Laboratory of Nuclear Physics and Ion-beam Application (MOE) - Fudan University, Shanghai, China

X. Gao³, H. Okawa

Zhejiang University, Hangzhou, China

M. Xiao

Universidad de Los Andes, Bogota, Colombia

C. Avila, A. Cabrera, C. Florez, J. Fraga, A. Sarkar, M.A. Segura Delgado

Universidad de Antioquia, Medellin, Colombia

J. Jaramillo, J. Mejia Guisao, F. Ramirez, J.D. Ruiz Alvarez, C.A. Salazar González, N. Vanegas Arbelaez

University of Split, Faculty of Electrical Engineering, Mechanical Engineering and Naval Architecture, Split, Croatia

D. Giljanovic, N. Godinovic, D. Lelas, I. Puljak

University of Split, Faculty of Science, Split, Croatia

Z. Antunovic, M. Kovac, T. Sculac

Institute Rudjer Boskovic, Zagreb, Croatia

V. Brigljevic, D. Ferencek, D. Majumder, M. Roguljic, A. Starodumov¹¹, T. Susa

University of Cyprus, Nicosia, Cyprus

M.W. Ather, A. Attikis, E. Erodou, A. Ioannou, G. Kole, M. Kolosova, S. Konstantinou, J. Mousa, C. Nicolaou, F. Ptochos, P.A. Razis, H. Rykaczewski, H. Saka, D. Tsiakkouri

Charles University, Prague, Czech Republic

M. Finger¹², M. Finger Jr.¹², A. Kveton, J. Tomsa

Escuela Politecnica Nacional, Quito, Ecuador

E. Ayala

Universidad San Francisco de Quito, Quito, Ecuador

E. Carrera Jarrin

Academy of Scientific Research and Technology of the Arab Republic of Egypt, Egyptian Network of High Energy Physics, Cairo, Egypt

S. Abu Zeid¹³, S. Elgammal¹⁴, E. Salama^{14,13}

Center for High Energy Physics (CHEP-FU), Fayoum University, El-Fayoum, Egypt

A. Lotfy, M.A. Mahmoud

National Institute of Chemical Physics and Biophysics, Tallinn, Estonia

S. Bhowmik, A. Carvalho Antunes De Oliveira, R.K. Dewanjee, K. Ehataht, M. Kadastik, J. Pata, M. Raidal, C. Veelken

Department of Physics, University of Helsinki, Helsinki, Finland

P. Eerola, L. Forthomme, H. Kirschenmann, K. Osterberg, M. Voutilainen

Helsinki Institute of Physics, Helsinki, Finland

E. Brücken, F. Garcia, J. Havukainen, V. Karimäki, M.S. Kim, R. Kinnunen, T. Lampén, K. Lassila-Perini, S. Lehti, T. Lindén, H. Siikonen, E. Tuominen, J. Tuominiemi

Lappeenranta University of Technology, Lappeenranta, Finland

P. Luukka, T. Tuuva

IRFU, CEA, Université Paris-Saclay, Gif-sur-Yvette, France

C. Amendola, M. Besancon, F. Couderc, M. Dejardin, D. Denegri, J.L. Faure, F. Ferri, S. Ganjour, A. Givernaud, P. Gras, G. Hamel de Monchenault, P. Jarry, B. Lenzi, E. Locci, J. Malcles, J. Rander, A. Rosowsky, M.Ö. Sahin, A. Savoy-Navarro¹⁵, M. Titov, G.B. Yu

Laboratoire Leprince-Ringuet, CNRS/IN2P3, Ecole Polytechnique, Institut Polytechnique de Paris, Palaiseau, France

S. Ahuja, F. Beaudette, M. Bonanomi, A. Buchot Perraguin, P. Busson, C. Charlot, O. Davignon, B. Diab, G. Falmagne, R. Granier de Cassagnac, A. Hakimi, I. Kucher, A. Lobanov, C. Martin Perez, M. Nguyen, C. Ochando, P. Paganini, J. Rembser, R. Salerno, J.B. Sauvan, Y. Sirois, A. Zabi, A. Zghiche

Université de Strasbourg, CNRS, IPHC UMR 7178, Strasbourg, France

J.-L. Agram¹⁶, J. Andrea, D. Bloch, G. Bourgatte, J.-M. Brom, E.C. Chabert, C. Collard, J.-C. Fontaine¹⁶, U. Goerlach, C. Grimault, A.-C. Le Bihan, P. Van Hove

Université de Lyon, Université Claude Bernard Lyon 1, CNRS-IN2P3, Institut de Physique Nucléaire de Lyon, Villeurbanne, France

E. Asilar, S. Beauceron, C. Bernet, G. Boudoul, C. Camen, A. Carle, N. Chanon, D. Contardo, P. Depasse, H. El Mamouni, J. Fay, S. Gascon, M. Gouzevitch, B. Ille, Sa. Jain, I.B. Laktineh, H. Lattaud, A. Lesauvage, M. Lethuillier, L. Mirabito, K. Shchablo, L. Torterotot, G. Touquet, M. Vander Donckt, S. Viret

Georgian Technical University, Tbilisi, Georgia

I. Bagaturia¹⁷, Z. Tsamalaidze¹²

RWTH Aachen University, I. Physikalisches Institut, Aachen, Germany

L. Feld, K. Klein, M. Lipinski, D. Meuser, A. Pauls, M.P. Rauch, J. Schulz, M. Teroerde

RWTH Aachen University, III. Physikalisches Institut A, Aachen, Germany

D. Eliseev, M. Erdmann, P. Fackeldey, B. Fischer, S. Ghosh, T. Hebbeker, K. Hoepfner, H. Keller, L. Mastrolorenzo, M. Merschmeyer, A. Meyer, G. Mocellin, S. Mondal, S. Mukherjee, D. Noll, A. Novak, T. Pook, A. Pozdnyakov, Y. Rath, H. Reithler, J. Roemer, A. Schmidt, S.C. Schuler, A. Sharma, S. Wiedenbeck, S. Zaleski

RWTH Aachen University, III. Physikalisches Institut B, Aachen, Germany

C. Dziwok, G. Flügge, W. Haj Ahmad¹⁸, O. Hlushchenko, T. Kress, A. Nowack, C. Pistone, O. Pooth, D. Roy, H. Sert, A. Stahl¹⁹, T. Ziemons

Deutsches Elektronen-Synchrotron, Hamburg, Germany

H. Aarup Petersen, M. Aldaya Martin, P. Asmuss, I. Babounikau, S. Baxter, O. Behnke, A. Bermúdez Martínez, A.A. Bin Anuar, K. Borras²⁰, V. Botta, D. Brunner, A. Campbell, A. Cardini, P. Connor, S. Consuegra Rodríguez, V. Danilov, A. De Wit, M.M. Defranchis, L. Didukh, D. Domínguez Damiani, G. Eckerlin, D. Eckstein, L.I. Estevez Banos, E. Gallo²¹, A. Geiser, A. Giraldi, A. Grohsjean, M. Guthoff, A. Harb, A. Jafari²², N.Z. Jomhari, H. Jung, A. Kasem²⁰, M. Kasemann, H. Kaveh, C. Kleinwort, J. Knolle, D. Krücker, W. Lange, T. Lenz, J. Lidrych, K. Lipka, W. Lohmann²³, T. Madlener, R. Mankel, I.-A. Melzer-Pellmann, J. Metwally, A.B. Meyer, M. Meyer, J. Mnich, A. Mussgiller, V. Myronenko, Y. Otari, D. Pérez Adán, S.K. Pflitsch, D. Pitzl, A. Raspereza, A. Saggio, A. Saibel, M. Savitskyi, V. Scheurer, C. Schwanenberger, A. Singh, R.E. Sosa Ricardo, N. Tonon, O. Turkot, A. Vagnerini, M. Van De Klundert, R. Walsh, D. Walter, Y. Wen, K. Wichmann, C. Wissing, S. Wuchterl, O. Zenaiev, R. Zlebcik

University of Hamburg, Hamburg, Germany

R. Aggleton, S. Bein, L. Benato, A. Benecke, K. De Leo, T. Dreyer, M. Eich, F. Feindt, A. Fröhlich, C. Garbers, E. Garutti, P. Gunnellini, J. Haller, A. Hinzmann, A. Karavdina, G. Kasieczka, R. Klanner, R. Kogler, V. Kutzner, J. Lange, T. Lange, A. Malara, C.E.N. Niemeyer, A. Nigamova, K.J. Pena Rodriguez, O. Rieger, P. Schleper, M. Schröder, S. Schumann, J. Schwandt, D. Schwarz, J. Sonneveld, H. Stadie, G. Steinbrück, A. Tews, B. Vormwald, I. Zoi

Karlsruher Institut fuer Technologie, Karlsruhe, Germany

J. Bechtel, T. Berger, E. Butz, R. Caspart, T. Chwalek, W. De Boer, A. Dierlamm, A. Droll, K. El Morabit, N. Faltermann, K. Flöh, M. Giffels, J.o. Gosewisch, A. Gottmann, F. Hartmann¹⁹, C. Heidecker, U. Husemann, I. Katkov²⁴, P. Keicher, R. Koppenhöfer, S. Maier, M. Metzler, S. Mitra, Th. Müller, M. Musich, M. Neukum, G. Quast, K. Rabbertz, J. Rauser, D. Savoii, D. Schäfer, M. Schnepf, D. Seith, I. Shvetsov, H.J. Simonis, R. Ulrich, J. Van Der Linden, R.F. Von Cube, M. Wassmer, M. Weber, S. Wieland, R. Wolf, S. Wozniewski, S. Wunsch

Institute of Nuclear and Particle Physics (INPP), NCSR Demokritos, Aghia Paraskevi, Greece

G. Anagnostou, P. Asenov, G. Daskalakis, T. Geralis, A. Kyriakis, D. Loukas, G. Paspalaki, A. Stakia

National and Kapodistrian University of Athens, Athens, Greece

M. Diamantopoulou, D. Karasavvas, G. Karathanasis, P. Kontaxakis, C.K. Koraka, A. Manousakis-katsikakis, A. Panagiotou, I. Papavergou, N. Saoulidou, K. Theofilatos, E. Tziaferi, K. Vellidis, E. Vourliotis

National Technical University of Athens, Athens, Greece

G. Bakas, K. Kousouris, I. Papakrivopoulos, G. Tsipolitis, A. Zacharopoulou

University of Ioánnina, Ioánnina, Greece

I. Evangelou, C. Foudas, P. Gianneios, P. Katsoulis, P. Kokkas, K. Manitaras, N. Manthos, I. Papadopoulos, J. Strologas

MTA-ELTE Lendület CMS Particle and Nuclear Physics Group, Eötvös Loránd University,

Budapest, Hungary

M. Csanad, M.M.A. Gadallah²⁵, S. Lökös²⁶, P. Major, K. Mandal, A. Mehta, G. Pasztor, O. Surányi, G.I. Veres

Wigner Research Centre for Physics, Budapest, Hungary

M. Bartók²⁷, G. Bencze, C. Hajdu, D. Horvath²⁸, F. Sikler, V. Veszpremi, G. Vesztergombi[†]

Institute of Nuclear Research ATOMKI, Debrecen, Hungary

S. Czellar, J. Karancsi²⁷, J. Molnar, Z. Szillasi, D. Teyssier

Institute of Physics, University of Debrecen, Debrecen, Hungary

P. Raics, Z.L. Trocsanyi²⁹, B. Ujvari

Eszterhazy Karoly University, Karoly Robert Campus, Gyongyos, Hungary

T. Csorgo³⁰, F. Nemes³⁰, T. Novak

Indian Institute of Science (IISc), Bangalore, India

S. Choudhury, J.R. Komaragiri, D. Kumar, L. Panwar, P.C. Tiwari

National Institute of Science Education and Research, HBNI, Bhubaneswar, India

S. Bahinipati³¹, D. Dash, C. Kar, P. Mal, T. Mishra, V.K. Muraleedharan Nair Bindhu³², A. Nayak³², N. Sur, S.K. Swain

Panjab University, Chandigarh, India

S. Bansal, S.B. Beri, V. Bhatnagar, G. Chaudhary, S. Chauhan, N. Dhingra³³, R. Gupta, A. Kaur, S. Kaur, P. Kumari, M. Meena, K. Sandeep, J.B. Singh, A.K. Viridi

University of Delhi, Delhi, India

A. Ahmed, A. Bhardwaj, B.C. Choudhary, R.B. Garg, M. Gola, S. Keshri, A. Kumar, M. Naimuddin, P. Priyanka, K. Ranjan, A. Shah

Saha Institute of Nuclear Physics, HBNI, Kolkata, India

M. Bharti³⁴, R. Bhattacharya, S. Bhattacharya, D. Bhowmik, S. Dutta, S. Ghosh, B. Gomber³⁵, M. Maity³⁶, S. Nandan, P. Palit, P.K. Rout, G. Saha, B. Sahu, S. Sarkar, M. Sharan, B. Singh³⁴, S. Thakur³⁴

Indian Institute of Technology Madras, Madras, India

P.K. Behera, S.C. Behera, P. Kalbhor, A. Muhammad, R. Pradhan, P.R. Pujahari, A. Sharma, A.K. Sikdar

Bhabha Atomic Research Centre, Mumbai, India

D. Dutta, V. Jha, V. Kumar, D.K. Mishra, K. Naskar³⁷, P.K. Netrakanti, L.M. Pant, P. Shukla

Tata Institute of Fundamental Research-A, Mumbai, India

T. Aziz, S. Dugad, G.B. Mohanty, U. Sarkar

Tata Institute of Fundamental Research-B, Mumbai, India

S. Banerjee, S. Bhattacharya, S. Chatterjee, R. Chudasama, M. Guchait, S. Karmakar, S. Kumar, G. Majumdar, K. Mazumdar, S. Mukherjee, D. Roy

Indian Institute of Science Education and Research (IISER), Pune, India

S. Dube, B. Kansal, S. Pandey, A. Rane, A. Rastogi, S. Sharma

Department of Physics, Isfahan University of Technology, Isfahan, Iran

H. Bakhshiansohi³⁸, M. Zeinali³⁹

Institute for Research in Fundamental Sciences (IPM), Tehran, IranS. Chenarani⁴⁰, S.M. Etesami, M. Khakzad, M. Mohammadi Najafabadi**University College Dublin, Dublin, Ireland**

M. Felcini, M. Grunewald

INFN Sezione di Bari ^a, Università di Bari ^b, Politecnico di Bari ^c, Bari, ItalyM. Abbrescia^{a,b}, R. Aly^{a,b,41}, C. Aruta^{a,b}, A. Colaleo^a, D. Creanza^{a,c}, N. De Filippis^{a,c}, M. De Palma^{a,b}, A. Di Florio^{a,b}, A. Di Pilato^{a,b}, W. Elmetenawee^{a,b}, L. Fiore^a, A. Gelmi^{a,b}, M. Gul^a, G. Iaselli^{a,c}, M. Ince^{a,b}, S. Lezki^{a,b}, G. Maggi^{a,c}, M. Maggi^a, I. Margjeka^{a,b}, V. Mastrapasqua^{a,b}, J.A. Merlin^a, S. My^{a,b}, S. Nuzzo^{a,b}, A. Pompili^{a,b}, G. Pugliese^{a,c}, A. Ranieri^a, G. Selvaggi^{a,b}, L. Silvestris^a, F.M. Simone^{a,b}, R. Venditti^a, P. Verwilligen^a**INFN Sezione di Bologna ^a, Università di Bologna ^b, Bologna, Italy**G. Abbiendi^a, C. Battilana^{a,b}, D. Bonacorsi^{a,b}, L. Borgonovi^a, S. Braibant-Giacomelli^{a,b}, R. Campanini^{a,b}, P. Capiluppi^{a,b}, A. Castro^{a,b}, F.R. Cavallo^a, C. Ciocca^a, M. Cuffiani^{a,b}, G.M. Dallavalle^a, T. Diotallevi^{a,b}, F. Fabbri^a, A. Fanfani^{a,b}, E. Fontanesi^{a,b}, P. Giacomelli^a, L. Giommi^{a,b}, C. Grandi^a, L. Guiducci^{a,b}, F. Iemmi^{a,b}, S. Lo Meo^{a,42}, S. Marcellini^a, G. Masetti^a, F.L. Navarria^{a,b}, A. Perrotta^a, F. Primavera^{a,b}, A.M. Rossi^{a,b}, T. Rovelli^{a,b}, G.P. Siroli^{a,b}, N. Tosi^a**INFN Sezione di Catania ^a, Università di Catania ^b, Catania, Italy**S. Albergo^{a,b,43}, S. Costa^{a,b}, A. Di Mattia^a, R. Potenza^{a,b}, A. Tricomi^{a,b,43}, C. Tuve^{a,b}**INFN Sezione di Firenze ^a, Università di Firenze ^b, Firenze, Italy**G. Barbagli^a, A. Cassese^a, R. Ceccarelli^{a,b}, V. Ciulli^{a,b}, C. Civinini^a, R. D'Alessandro^{a,b}, F. Fiori^a, E. Focardi^{a,b}, G. Latino^{a,b}, P. Lenzi^{a,b}, M. Lizzo^{a,b}, M. Meschini^a, S. Paoletti^a, R. Seidita^{a,b}, G. Sguazzoni^a, L. Viliani^a**INFN Laboratori Nazionali di Frascati, Frascati, Italy**

L. Benussi, S. Bianco, D. Piccolo

INFN Sezione di Genova ^a, Università di Genova ^b, Genova, ItalyM. Bozzo^{a,b}, F. Ferro^a, R. Mulargia^{a,b}, E. Robutti^a, S. Tosi^{a,b}**INFN Sezione di Milano-Bicocca ^a, Università di Milano-Bicocca ^b, Milano, Italy**A. Benaglia^a, A. Beschi^{a,b}, F. Brivio^{a,b}, F. Cetorelli^{a,b}, V. Ciriolo^{a,b,19}, F. De Guio^{a,b}, M.E. Dinardo^{a,b}, P. Dini^a, S. Gennai^a, A. Ghezzi^{a,b}, P. Govoni^{a,b}, L. Guzzi^{a,b}, M. Malberti^a, S. Malvezzi^a, A. Massironi^a, D. Menasce^a, F. Monti^{a,b}, L. Moroni^a, M. Paganoni^{a,b}, D. Pedrini^a, S. Ragazzi^{a,b}, T. Tabarelli de Fatis^{a,b}, D. Valsecchi^{a,b,19}, D. Zuolo^{a,b}**INFN Sezione di Napoli ^a, Università di Napoli 'Federico II' ^b, Napoli, Italy, Università della Basilicata ^c, Potenza, Italy, Università G. Marconi ^d, Roma, Italy**S. Buontempo^a, N. Cavallo^{a,c}, A. De Iorio^{a,b}, F. Fabozzi^{a,c}, F. Fienga^a, A.O.M. Iorio^{a,b}, L. Lista^{a,b}, S. Meola^{a,d,19}, P. Paolucci^{a,19}, B. Rossi^a, C. Sciacca^{a,b}**INFN Sezione di Padova ^a, Università di Padova ^b, Padova, Italy, Università di Trento ^c, Trento, Italy**P. Azzi^a, N. Bacchetta^a, D. Bisello^{a,b}, P. Bortignon^a, A. Bragagnolo^{a,b}, R. Carlin^{a,b}, P. Checchia^a, P. De Castro Manzano^a, T. Dorigo^a, F. Gasparini^{a,b}, U. Gasparini^{a,b}, S.Y. Hoh^{a,b}, L. Layer^{a,44}, M. Margoni^{a,b}, A.T. Meneguzzo^{a,b}, M. Presilla^{a,b}, P. Ronchese^{a,b}, R. Rossin^{a,b}, F. Simonetto^{a,b}, G. Strong^a, M. Tosi^{a,b}, H. YARAR^{a,b}, M. Zanetti^{a,b}, P. Zotto^{a,b}, A. Zucchetta^{a,b}, G. Zumerle^{a,b}**INFN Sezione di Pavia ^a, Università di Pavia ^b, Pavia, Italy**C. Aime^{a,b}, A. Braghieri^a, S. Calzaferri^{a,b}, D. Fiorina^{a,b}, P. Montagna^{a,b}, S.P. Ratti^{a,b}, V. Re^a, M. Ressegotti^{a,b}, C. Riccardi^{a,b}, P. Salvini^a, I. Vai^a, P. Vitulo^{a,b}

INFN Sezione di Perugia ^a, Università di Perugia ^b, Perugia, Italy

G.M. Bilei^a, D. Ciangottini^{a,b}, L. Fanò^{a,b}, P. Lariccia^{a,b}, G. Mantovani^{a,b}, V. Mariani^{a,b}, M. Menichelli^a, F. Moscatelli^a, A. Piccinelli^{a,b}, A. Rossi^{a,b}, A. Santocchia^{a,b}, D. Spiga^a, T. Tedeschi^{a,b}

INFN Sezione di Pisa ^a, Università di Pisa ^b, Scuola Normale Superiore di Pisa ^c, Pisa Italy, Università di Siena ^d, Siena, Italy

K. Androsov^a, P. Azzurri^a, G. Bagliesi^a, V. Bertacchi^{a,c}, L. Bianchini^a, T. Boccali^a, E. Bossini, R. Castaldi^a, M.A. Ciocci^{a,b}, R. Dell'Orso^a, M.R. Di Domenico^{a,d}, S. Donato^a, A. Giassi^a, M.T. Grippo^a, F. Ligabue^{a,c}, E. Manca^{a,c}, G. Mandorli^{a,c}, A. Messineo^{a,b}, F. Palla^a, G. Ramirez-Sanchez^{a,c}, A. Rizzi^{a,b}, G. Rolandi^{a,c}, S. Roy Chowdhury^{a,c}, A. Scribano^a, N. Shafiei^{a,b}, P. Spagnolo^a, R. Tenchini^a, G. Tonelli^{a,b}, N. Turini^{a,d}, A. Venturi^a, P.G. Verdini^a

INFN Sezione di Roma ^a, Sapienza Università di Roma ^b, Rome, Italy

F. Cavallari^a, M. Cipriani^{a,b}, D. Del Re^{a,b}, E. Di Marco^a, M. Diemoz^a, E. Longo^{a,b}, P. Meridiani^a, G. Organtini^{a,b}, F. Pandolfi^a, R. Paramatti^{a,b}, C. Quaranta^{a,b}, S. Rahatlou^{a,b}, C. Rovelli^a, F. Santanastasio^{a,b}, L. Soffi^{a,b}, R. Tramontano^{a,b}

INFN Sezione di Torino ^a, Università di Torino ^b, Torino, Italy, Università del Piemonte Orientale ^c, Novara, Italy

N. Amapane^{a,b}, R. Arcidiacono^{a,c}, S. Argiro^{a,b}, M. Arneodo^{a,c}, N. Bartosik^a, R. Bellan^{a,b}, A. Bellora^{a,b}, J. Berenguer Antequera^{a,b}, C. Biino^a, A. Cappati^{a,b}, N. Cartiglia^a, S. Cometti^a, M. Costa^{a,b}, R. Covarelli^{a,b}, N. Demaria^a, B. Kiani^{a,b}, F. Legger^a, C. Mariotti^a, S. Maselli^a, E. Migliore^{a,b}, V. Monaco^{a,b}, E. Monteil^{a,b}, M. Monteno^a, M.M. Obertino^{a,b}, G. Ortona^a, L. Pacher^{a,b}, N. Pastrone^a, M. Pelliccioni^a, G.L. Pinna Angioni^{a,b}, M. Ruspa^{a,c}, R. Salvatico^{a,b}, F. Siviero^{a,b}, V. Sola^a, A. Solano^{a,b}, D. Soldi^{a,b}, A. Staiano^a, M. Tornago^{a,b}, D. Trocino^{a,b}

INFN Sezione di Trieste ^a, Università di Trieste ^b, Trieste, Italy

S. Belforte^a, V. Candelise^{a,b}, M. Casarsa^a, F. Cossutti^a, A. Da Rold^{a,b}, G. Della Ricca^{a,b}, F. Vazzoler^{a,b}

Kyungpook National University, Daegu, Korea

S. Dogra, C. Huh, B. Kim, D.H. Kim, G.N. Kim, J. Lee, S.W. Lee, C.S. Moon, Y.D. Oh, S.I. Pak, B.C. Radburn-Smith, S. Sekmen, Y.C. Yang

Chonnam National University, Institute for Universe and Elementary Particles, Kwangju, Korea

H. Kim, D.H. Moon

Hanyang University, Seoul, Korea

B. Francois, T.J. Kim, J. Park

Korea University, Seoul, Korea

S. Cho, S. Choi, Y. Go, B. Hong, K. Lee, K.S. Lee, J. Lim, J. Park, S.K. Park, J. Yoo

Kyung Hee University, Department of Physics, Seoul, Republic of Korea

J. Goh, A. Gurtu

Sejong University, Seoul, Korea

H.S. Kim, Y. Kim

Seoul National University, Seoul, Korea

J. Almond, J.H. Bhyun, J. Choi, S. Jeon, J. Kim, J.S. Kim, S. Ko, H. Kwon, H. Lee, S. Lee, K. Nam, B.H. Oh, M. Oh, S.B. Oh, H. Seo, U.K. Yang, I. Yoon

University of Seoul, Seoul, Korea

D. Jeon, J.H. Kim, B. Ko, J.S.H. Lee, I.C. Park, Y. Roh, D. Song, I.J. Watson

Yonsei University, Department of Physics, Seoul, Korea

S. Ha, H.D. Yoo

Sungkyunkwan University, Suwon, Korea

Y. Choi, C. Hwang, Y. Jeong, H. Lee, Y. Lee, I. Yu

College of Engineering and Technology, American University of the Middle East (AUM), Dasman, Kuwait

Y. Maghrbi

Riga Technical University, Riga, Latvia

V. Veckalns⁴⁵

Vilnius University, Vilnius, Lithuania

M. Ambrozas, A. Juodagalvis, A. Rinkevicius, G. Tamulaitis, A. Vaitkevicius

National Centre for Particle Physics, Universiti Malaya, Kuala Lumpur, Malaysia

W.A.T. Wan Abdullah, M.N. Yusli, Z. Zolkapli

Universidad de Sonora (UNISON), Hermosillo, Mexico

J.F. Benitez, A. Castaneda Hernandez, J.A. Murillo Quijada, L. Valencia Palomo

Centro de Investigacion y de Estudios Avanzados del IPN, Mexico City, Mexico

G. Ayala, H. Castilla-Valdez, E. De La Cruz-Burelo, I. Heredia-De La Cruz⁴⁶, R. Lopez-Fernandez, C.A. Mondragon Herrera, D.A. Perez Navarro, A. Sanchez-Hernandez

Universidad Iberoamericana, Mexico City, Mexico

S. Carrillo Moreno, C. Oropeza Barrera, M. Ramirez-Garcia, F. Vazquez Valencia

Benemerita Universidad Autonoma de Puebla, Puebla, Mexico

I. Pedraza, H.A. Salazar Ibarguen, C. Uribe Estrada

University of Montenegro, Podgorica, Montenegro

J. Mijuskovic⁴, N. Raicevic

University of Auckland, Auckland, New Zealand

D. Krofcheck

University of Canterbury, Christchurch, New Zealand

S. Bheesette, P.H. Butler

National Centre for Physics, Quaid-I-Azam University, Islamabad, Pakistan

A. Ahmad, M.I. Asghar, A. Awais, M.I.M. Awan, H.R. Hoorani, W.A. Khan, M.A. Shah, M. Shoaib, M. Waqas

AGH University of Science and Technology Faculty of Computer Science, Electronics and Telecommunications, Krakow, Poland

V. Avati, L. Grzanka, M. Malawski

National Centre for Nuclear Research, Swierk, Poland

H. Bialkowska, M. Bluj, B. Boimska, T. Frueboes, M. Górski, M. Kazana, M. Szleper, P. Traczyk, P. Zalewski

Institute of Experimental Physics, Faculty of Physics, University of Warsaw, Warsaw, Poland

K. Bunkowski, K. Doroba, A. Kalinowski, M. Konecki, J. Krolikowski, M. Walczak

Laboratório de Instrumentação e Física Experimental de Partículas, Lisboa, Portugal

M. Araujo, P. Bargassa, D. Bastos, A. Boletti, P. Faccioli, M. Gallinaro, J. Hollar, N. Leonardo, T. Niknejad, J. Seixas, K. Shchelina, O. Toldaiev, J. Varela

Joint Institute for Nuclear Research, Dubna, Russia

S. Afanasiev, D. Budkouski, P. Bunin, M. Gavrilenko, I. Golutvin, I. Gorbunov, A. Kamenev, V. Karjavine, A. Lanev, A. Malakhov, V. Matveev^{47,48}, V. Palichik, V. Perelygin, M. Savina, D. Seitova, V. Shalaev, S. Shmatov, S. Shulha, V. Smirnov, O. Teryaev, N. Voytishin, A. Zarubin, I. Zhizhin

Petersburg Nuclear Physics Institute, Gatchina (St. Petersburg), Russia

G. Gavrilo, V. Golovtsov, Y. Ivanov, V. Kim⁴⁹, E. Kuznetsova⁵⁰, V. Murzin, V. Oreshkin, I. Smirnov, D. Sosnov, V. Sulimov, L. Uvarov, S. Volkov, A. Vorobyev

Institute for Nuclear Research, Moscow, Russia

Yu. Andreev, A. Dermenev, S. Gninenko, N. Golubev, A. Karneyeu, M. Kirsanov, N. Krasnikov, A. Pashenkov, G. Pivovarov, D. Tlisov[†], A. Toropin

Institute for Theoretical and Experimental Physics named by A.I. Alikhanov of NRC 'Kurchatov Institute', Moscow, Russia

V. Epshteyn, V. Gavrilo, N. Lychkovskaya, A. Nikitenko⁵¹, V. Popov, G. Safronov, A. Spiridonov, A. Stepenov, M. Toms, E. Vlasov, A. Zhokin

Moscow Institute of Physics and Technology, Moscow, Russia

T. Aushev

National Research Nuclear University 'Moscow Engineering Physics Institute' (MEPhI), Moscow, Russia

O. Bychkova, M. Chadeeva⁵², D. Philippov, E. Popova, V. Rusinov

P.N. Lebedev Physical Institute, Moscow, Russia

V. Andreev, M. Azarkin, I. Dremin, M. Kirakosyan, A. Terkulov

Skobeltsyn Institute of Nuclear Physics, Lomonosov Moscow State University, Moscow, Russia

A. Belyaev, E. Boos, M. Dubinin⁵³, L. Dudko, A. Ershov, A. Gribushin, V. Klyukhin, O. Kodolova, I. Lokhtin, S. Obraztsov, S. Petrushanko, V. Savrin, A. Snigirev

Novosibirsk State University (NSU), Novosibirsk, Russia

V. Blinov⁵⁴, T. Dimova⁵⁴, L. Kardapoltsev⁵⁴, I. Ovtin⁵⁴, Y. Skovpen⁵⁴

Institute for High Energy Physics of National Research Centre 'Kurchatov Institute', Protvino, Russia

I. Azhgirey, I. Bayshev, V. Kachanov, A. Kalinin, D. Konstantinov, V. Petrov, R. Ryutin, A. Sobol, S. Troshin, N. Tyurin, A. Uzunian, A. Volkov

National Research Tomsk Polytechnic University, Tomsk, Russia

A. Babaev, A. Iuzhakov, V. Okhotnikov, L. Sukhikh

Tomsk State University, Tomsk, Russia

V. Borchsh, V. Ivanchenko, E. Tcherniaev

University of Belgrade: Faculty of Physics and VINCA Institute of Nuclear Sciences, Belgrade, Serbia

P. Adzic⁵⁵, M. Dordevic, P. Milenovic, J. Milosevic

Centro de Investigaciones Energéticas Medioambientales y Tecnológicas (CIEMAT), Madrid, Spain

M. Aguilar-Benitez, J. Alcaraz Maestre, A. Álvarez Fernández, I. Bachiller, M. Barrio Luna, Cristina F. Bedoya, C.A. Carrillo Montoya, M. Cepeda, M. Cerrada, N. Colino, B. De La Cruz, A. Delgado Peris, J.P. Fernández Ramos, J. Flix, M.C. Fouz, O. Gonzalez Lopez, S. Goy Lopez, J.M. Hernandez, M.I. Josa, J. León Holgado, D. Moran, Á. Navarro Tobar, A. Pérez-Calero Yzquierdo, J. Puerta Pelayo, I. Redondo, L. Romero, S. Sánchez Navas, M.S. Soares, L. Urda Gómez, C. Willmott

Universidad Autónoma de Madrid, Madrid, Spain

C. Albajar, J.F. de Trocóniz, R. Reyes-Almanza

Universidad de Oviedo, Instituto Universitario de Ciencias y Tecnologías Espaciales de Asturias (ICTEA), Oviedo, Spain

B. Alvarez Gonzalez, J. Cuevas, C. Erice, J. Fernandez Menendez, S. Folgueras, I. Gonzalez Caballero, E. Palencia Cortezon, C. Ramón Álvarez, J. Ripoll Sau, V. Rodríguez Bouza, S. Sanchez Cruz, A. Trapote

Instituto de Física de Cantabria (IFCA), CSIC-Universidad de Cantabria, Santander, Spain

J.A. Brochero Cifuentes, I.J. Cabrillo, A. Calderon, B. Chazin Quero, J. Duarte Campderros, M. Fernandez, C. Fernandez Madrazo, P.J. Fernández Manteca, A. García Alonso, G. Gomez, C. Martinez Rivero, P. Martinez Ruiz del Arbol, F. Matorras, J. Piedra Gomez, C. Prieels, F. Ricci-Tam, T. Rodrigo, A. Ruiz-Jimeno, L. Scodellaro, N. Trevisani, I. Vila, J.M. Vizán Garcia

University of Colombo, Colombo, Sri Lanka

MK Jayananda, B. Kailasapathy⁵⁶, D.U.J. Sonnadara, DDC Wickramarathna

University of Ruhuna, Department of Physics, Matara, Sri Lanka

W.G.D. Dharmaratna, K. Liyanage, N. Perera, N. Wickramage

CERN, European Organization for Nuclear Research, Geneva, Switzerland

T.K. Aarrestad, D. Abbaneo, E. Auffray, G. Auzinger, J. Baechler, P. Baillon, A.H. Ball, D. Barney, J. Bendavid, N. Beni, M. Bianco, A. Bocci, E. Brondolin, T. Camporesi, M. Capeans Garrido, G. Cerminara, S.S. Chhibra, L. Cristella, D. d'Enterria, A. Dabrowski, N. Daci, A. David, A. De Roeck, M. Deile, R. Di Maria, M. Dobson, M. Dünser, N. Dupont, A. Elliott-Peisert, N. Emriskova, F. Fallavollita⁵⁷, D. Fasanella, S. Fiorendi, A. Florent, G. Franzoni, J. Fulcher, W. Funk, S. Giani, D. Gigi, K. Gill, F. Glege, L. Gouskos, M. Guilbaud, M. Haranko, J. Hegeman, Y. Iiyama, V. Innocente, T. James, P. Janot, J. Kaspar, J. Kieseler, M. Komm, N. Kratochwil, C. Lange, S. Laurila, P. Lecoq, K. Long, C. Lourenço, L. Malgeri, S. Mallios, M. Mannelli, F. Meijers, S. Mersi, E. Meschi, F. Moortgat, M. Mulders, S. Orfanelli, L. Orsini, F. Pantaleo¹⁹, L. Pape, E. Perez, M. Peruzzi, A. Petrilli, G. Petrucciani, A. Pfeiffer, M. Pierini, T. Quast, D. Rabaday, A. Racz, M. Rieger, M. Rovere, H. Sakulin, J. Salfeld-Nebgen, S. Scarfi, C. Schäfer, C. Schwick, M. Selvaggi, A. Sharma, P. Silva, W. Snoeys, P. Sphicas⁵⁸, S. Summers, V.R. Tavolaro, D. Treille, A. Tsiros, G.P. Van Onsem, M. Verzetti, K.A. Wozniak, W.D. Zeuner

Paul Scherrer Institut, Villigen, Switzerland

L. Caminada⁵⁹, A. Ebrahimi, W. Erdmann, R. Horisberger, Q. Ingram, H.C. Kaestli, D. Kotlinski, U. Langenegger, M. Missiroli, T. Rohe

ETH Zurich - Institute for Particle Physics and Astrophysics (IPA), Zurich, Switzerland

M. Backhaus, P. Berger, A. Calandri, N. Chernyavskaya, A. De Cosa, G. Dissertori, M. Dittmar, M. Donegà, C. Dorfer, T. Gadek, T.A. Gómez Espinosa, C. Grab, D. Hits, W. Lustermann, A.-M. Lyon, R.A. Manzoni, M.T. Meinhard, F. Micheli, F. Nessi-Tedaldi, J. Niedziela, F. Pauss,

V. Perovic, G. Perrin, S. Pigazzini, M.G. Ratti, M. Reichmann, C. Reissel, T. Reitenspiess, B. Ristic, D. Ruini, D.A. Sanz Becerra, M. Schönenberger, V. Stampf, J. Steggemann⁶⁰, R. Wallny, D.H. Zhu

Universität Zürich, Zurich, Switzerland

C. Amsler⁶¹, C. Botta, D. Brzhechko, M.F. Canelli, R. Del Burgo, J.K. Heikkilä, M. Huwiler, A. Jofrehei, B. Kilminster, S. Leontsinis, A. Macchiolo, P. Meiring, V.M. Mikuni, U. Molinatti, I. Neutelings, G. Rauco, A. Reimers, P. Robmann, K. Schweiger, Y. Takahashi

National Central University, Chung-Li, Taiwan

C. Adloff⁶², C.M. Kuo, W. Lin, A. Roy, T. Sarkar³⁶, S.S. Yu

National Taiwan University (NTU), Taipei, Taiwan

L. Ceard, P. Chang, Y. Chao, K.F. Chen, P.H. Chen, W.-S. Hou, Y.y. Li, R.-S. Lu, E. Paganis, A. Psallidas, A. Steen, E. Yazgan

Chulalongkorn University, Faculty of Science, Department of Physics, Bangkok, Thailand

B. Asavapibhop, C. Asawatangtrakuldee, N. Srimanobhas

Çukurova University, Physics Department, Science and Art Faculty, Adana, Turkey

F. Boran, S. Damaraseckin⁶³, Z.S. Demiroglu, F. Dolek, C. Dozen⁶⁴, I. Dumanoglu⁶⁵, E. Eskut, G. Gokbulut, Y. Guler, E. Gurpinar Guler⁶⁶, I. Hos⁶⁷, C. Isik, E.E. Kangal⁶⁸, O. Kara, A. Kayis Topaksu, U. Kiminsu, G. Onengut, K. Ozdemir⁶⁹, A. Polatoz, A.E. Simsek, B. Tali⁷⁰, U.G. Tok, S. Turkcapar, I.S. Zorbakir, C. Zorbilmez

Middle East Technical University, Physics Department, Ankara, Turkey

B. Isildak⁷¹, G. Karapinar⁷², K. Ocalan⁷³, M. Yalvac⁷⁴

Bogazici University, Istanbul, Turkey

B. Akgun, I.O. Atakisi, E. Gülmez, M. Kaya⁷⁵, O. Kaya⁷⁶, Ö. Özçelik, S. Tekten⁷⁷, E.A. Yetkin⁷⁸

Istanbul Technical University, Istanbul, Turkey

A. Cakir, K. Cankocak⁶⁵, Y. Komurcu, S. Sen⁷⁹

Istanbul University, Istanbul, Turkey

F. Aydogmus Sen, S. Cerci⁷⁰, B. Kaynak, S. Ozkorucuklu, D. Sunar Cerci⁷⁰

Institute for Scintillation Materials of National Academy of Science of Ukraine, Kharkov, Ukraine

B. Grynyov

National Scientific Center, Kharkov Institute of Physics and Technology, Kharkov, Ukraine

L. Levchuk

University of Bristol, Bristol, United Kingdom

E. Bhal, S. Bologna, J.J. Brooke, A. Bundock, E. Clement, D. Cussans, H. Flacher, J. Goldstein, G.P. Heath, H.F. Heath, L. Kreczko, B. Krikler, S. Paramesvaran, T. Sakuma, S. Seif El Nasr-Storey, V.J. Smith, N. Stylianou⁸⁰, J. Taylor, A. Titterton

Rutherford Appleton Laboratory, Didcot, United Kingdom

K.W. Bell, A. Belyaev⁸¹, C. Brew, R.M. Brown, D.J.A. Cockerill, K.V. Ellis, K. Harder, S. Harper, J. Linacre, K. Manolopoulos, D.M. Newbold, E. Olaiya, D. Petyt, T. Reis, T. Schuh, C.H. Shepherd-Themistocleous, A. Thea, I.R. Tomalin, T. Williams

Imperial College, London, United Kingdom

R. Bainbridge, P. Bloch, S. Bonomally, J. Borg, S. Breeze, O. Buchmuller, V. Cepaitis,

G.S. Chahal⁸², D. Colling, P. Dauncey, G. Davies, M. Della Negra, G. Fedi, G. Hall, G. Iles, J. Langford, L. Lyons, A.-M. Magnan, S. Malik, A. Martelli, V. Milosevic, J. Nash⁸³, V. Palladino, M. Pesaresi, D.M. Raymond, A. Richards, A. Rose, E. Scott, C. Seez, A. Shtipliyski, A. Tapper, K. Uchida, T. Virdee¹⁹, N. Wardle, S.N. Webb, D. Winterbottom, A.G. Zecchinelli

Brunel University, Uxbridge, United Kingdom

J.E. Cole, A. Khan, P. Kyberd, C.K. Mackay, I.D. Reid, L. Teodorescu, S. Zahid

Baylor University, Waco, USA

S. Abdullin, A. Brinkerhoff, K. Call, B. Caraway, J. Dittmann, K. Hatakeyama, A.R. Kanuganti, B. McMaster, N. Pastika, S. Sawant, C. Smith, C. Sutantawibul, J. Wilson

Catholic University of America, Washington, DC, USA

R. Bartek, A. Dominguez, R. Uniyal, A.M. Vargas Hernandez

The University of Alabama, Tuscaloosa, USA

A. Buccilli, O. Charaf, S.I. Cooper, D. Di Croce, S.V. Gleyzer, C. Henderson, C.U. Perez, P. Rumerio, C. West

Boston University, Boston, USA

A. Akpinar, A. Albert, D. Arcaro, C. Cosby, Z. Demiragli, D. Gastler, J. Rohlf, K. Salyer, D. Sperka, D. Spitzbart, I. Suarez, S. Yuan, D. Zou

Brown University, Providence, USA

G. Benelli, B. Burkle, X. Coubez²⁰, D. Cutts, Y.t. Duh, M. Hadley, U. Heintz, J.M. Hogan⁸⁴, K.H.M. Kwok, E. Laird, G. Landsberg, K.T. Lau, J. Lee, J. Luo, M. Narain, S. Sagir⁸⁵, E. Usai, W.Y. Wong, X. Yan, D. Yu, W. Zhang

University of California, Davis, Davis, USA

R. Band, C. Brainerd, R. Breedon, M. Calderon De La Barca Sanchez, M. Chertok, J. Conway, R. Conway, P.T. Cox, R. Erbacher, C. Flores, F. Jensen, O. Kukral, R. Lander, M. Mulhearn, D. Pellett, M. Shi, D. Taylor, M. Tripathi, Y. Yao, F. Zhang

University of California, Los Angeles, USA

M. Bachtis, R. Cousins, A. Dasgupta, A. Datta, D. Hamilton, J. Hauser, M. Ignatenko, M.A. Iqbal, T. Lam, N. Mccoll, W.A. Nash, S. Regnard, D. Saltzberg, C. Schnaible, B. Stone, V. Valuev

University of California, Riverside, Riverside, USA

K. Burt, Y. Chen, R. Clare, J.W. Gary, G. Hanson, G. Karapostoli, O.R. Long, N. Manganeli, M. Olmedo Negrete, W. Si, S. Wimpenny, Y. Zhang

University of California, San Diego, La Jolla, USA

J.G. Branson, P. Chang, S. Cittolin, S. Cooperstein, N. Deelen, J. Duarte, R. Gerosa, L. Giannini, D. Gilbert, V. Krutelyov, J. Letts, M. Masciovecchio, S. May, S. Padhi, M. Pieri, V. Sharma, M. Tadel, A. Vartak, F. Würthwein, A. Yagil

University of California, Santa Barbara - Department of Physics, Santa Barbara, USA

N. Amin, C. Campagnari, M. Citron, A. Dorsett, V. Dutta, J. Incandela, M. Kilpatrick, B. Marsh, H. Mei, A. Ovcharova, H. Qu, M. Quinnan, J. Richman, U. Sarica, D. Stuart, S. Wang

California Institute of Technology, Pasadena, USA

A. Bornheim, O. Cerri, I. Dutta, J.M. Lawhorn, N. Lu, J. Mao, H.B. Newman, J. Ngadiuba, T.Q. Nguyen, M. Spiropulu, J.R. Vlimant, C. Wang, S. Xie, Z. Zhang, R.Y. Zhu

Carnegie Mellon University, Pittsburgh, USA

J. Alison, M.B. Andrews, T. Ferguson, T. Mudholkar, M. Paulini, I. Vorobiev

University of Colorado Boulder, Boulder, USA

J.P. Cumalat, W.T. Ford, E. MacDonald, R. Patel, A. Perloff, K. Stenson, K.A. Ulmer, S.R. Wagner

Cornell University, Ithaca, USA

J. Alexander, Y. Cheng, J. Chu, D.J. Cranshaw, K. Mcdermott, J. Monroy, J.R. Patterson, D. Quach, A. Ryd, W. Sun, S.M. Tan, Z. Tao, J. Thom, P. Wittich, M. Zientek

Fermi National Accelerator Laboratory, Batavia, USA

M. Albrow, M. Alyari, G. Apollinari, A. Apresyan, A. Apyan, S. Banerjee, L.A.T. Bauerdick, A. Beretvas, D. Berry, J. Berryhill, P.C. Bhat, K. Burkett, J.N. Butler, A. Canepa, G.B. Cerati, H.W.K. Cheung, F. Chlebana, M. Cremonesi, K.F. Di Petrillo, V.D. Elvira, J. Freeman, Z. Gecse, L. Gray, D. Green, S. Grünendahl, O. Gutsche, R.M. Harris, R. Heller, T.C. Herwig, J. Hirschauer, B. Jayatilaka, S. Jindariani, M. Johnson, U. Joshi, P. Klabbers, T. Klijnsma, B. Klima, M.J. Kortelainen, S. Lammel, D. Lincoln, R. Lipton, T. Liu, J. Lykken, C. Madrid, K. Maeshima, C. Mantilla, D. Mason, P. McBride, P. Merkel, S. Mrenna, S. Nahn, V. O'Dell, V. Papadimitriou, K. Pedro, C. Pena⁵³, O. Prokofyev, F. Ravera, A. Reinsvold Hall, L. Ristori, B. Schneider, E. Sexton-Kennedy, N. Smith, A. Soha, L. Spiegel, S. Stoynev, J. Strait, L. Taylor, S. Tkaczyk, N.V. Tran, L. Uplegger, E.W. Vaandering, H.A. Weber

University of Florida, Gainesville, USA

D. Acosta, P. Avery, D. Bourilkov, L. Cadamuro, V. Cherepanov, F. Errico, R.D. Field, D. Guerrero, B.M. Joshi, M. Kim, J. Konigsberg, A. Korytov, K.H. Lo, K. Matchev, N. Menendez, G. Mitselmakher, D. Rosenzweig, K. Shi, J. Sturdy, J. Wang, E. Yigitbasi, X. Zuo

Florida State University, Tallahassee, USA

T. Adams, A. Askew, D. Diaz, R. Habibullah, S. Hagopian, V. Hagopian, K.F. Johnson, R. Khurana, T. Kolberg, G. Martinez, H. Prosper, C. Schiber, R. Yohay, J. Zhang

Florida Institute of Technology, Melbourne, USA

M.M. Baarmand, S. Butalla, T. Elkafrawy¹³, M. Hohlmann, R. Kumar Verma, D. Noonan, M. Rahmani, M. Saunders, F. Yumiceva

University of Illinois at Chicago (UIC), Chicago, USA

M.R. Adams, L. Apanasevich, H. Becerril Gonzalez, R. Cavanaugh, X. Chen, S. Dittmer, O. Evdokimov, C.E. Gerber, D.A. Hangal, D.J. Hofman, C. Mills, G. Oh, T. Roy, M.B. Tonjes, N. Varelas, J. Viinikainen, X. Wang, Z. Wu, Z. Ye

The University of Iowa, Iowa City, USA

M. Alhusseini, K. Dilsiz⁸⁶, S. Durgut, R.P. Gandrajula, M. Haytmyradov, V. Khristenko, O.K. Köseyan, J.-P. Merlo, A. Mestvirishvili⁸⁷, A. Moeller, J. Nachtman, H. Ogul⁸⁸, Y. Onel, F. Ozok⁸⁹, A. Penzo, C. Snyder, E. Tiras⁹⁰, J. Wetzel

Johns Hopkins University, Baltimore, USA

O. Amram, B. Blumenfeld, L. Corcodilos, M. Eminizer, A.V. Gritsan, S. Kyriacou, P. Maksimovic, J. Roskes, M. Swartz, T.Á. Vami

The University of Kansas, Lawrence, USA

C. Baldenegro Barrera, P. Baringer, A. Bean, A. Bylinkin, T. Isidori, S. Khalil, J. King, G. Krintiras, A. Kropivnitskaya, C. Lindsey, N. Minafra, M. Murray, C. Rogan, C. Royon, S. Sanders, E. Schmitz, J.D. Tapia Takaki, Q. Wang, J. Williams, G. Wilson

Kansas State University, Manhattan, USA

S. Duric, A. Ivanov, K. Kaadze, D. Kim, Y. Maravin, T. Mitchell, A. Modak

Lawrence Livermore National Laboratory, Livermore, USA

F. Rebassoo, D. Wright

University of Maryland, College Park, USA

E. Adams, A. Baden, O. Baron, A. Belloni, S.C. Eno, Y. Feng, N.J. Hadley, S. Jabeen, R.G. Kellogg, T. Koeth, A.C. Mignerey, S. Nabili, M. Seidel, A. Skuja, S.C. Tonwar, L. Wang, K. Wong

Massachusetts Institute of Technology, Cambridge, USA

D. Abercrombie, R. Bi, S. Brandt, W. Busza, I.A. Cali, Y. Chen, M. D'Alfonso, G. Gomez Ceballos, M. Goncharov, P. Harris, M. Hu, M. Klute, D. Kovalskyi, J. Krupa, Y.-J. Lee, P.D. Luckey, B. Maier, A.C. Marini, C. Mironov, X. Niu, C. Paus, D. Rankin, C. Roland, G. Roland, Z. Shi, G.S.F. Stephans, K. Tatar, D. Velicanu, J. Wang, T.W. Wang, Z. Wang, B. Wyslouch

University of Minnesota, Minneapolis, USA

R.M. Chatterjee, A. Evans, P. Hansen, J. Hiltbrand, Sh. Jain, M. Krohn, Y. Kubota, Z. Lesko, J. Mans, M. Revering, R. Rusack, R. Saradhy, N. Schroeder, N. Strobbe, M.A. Wadud

University of Mississippi, Oxford, USA

J.G. Acosta, S. Oliveros

University of Nebraska-Lincoln, Lincoln, USA

K. Bloom, M. Bryson, S. Chauhan, D.R. Claes, C. Fangmeier, L. Finco, F. Golf, J.R. González Fernández, C. Joo, I. Kravchenko, J.E. Siado, G.R. Snow[†], W. Tabb, F. Yan

State University of New York at Buffalo, Buffalo, USA

G. Agarwal, H. Bandyopadhyay, L. Hay, I. Iashvili, A. Kharchilava, C. McLean, D. Nguyen, J. Pekkanen, S. Rappoccio

Northeastern University, Boston, USA

G. Alverson, E. Barberis, C. Freer, Y. Haddad, A. Hortiangtham, J. Li, G. Madigan, B. Marzocchi, D.M. Morse, V. Nguyen, T. Orimoto, A. Parker, L. Skinnari, A. Tishelman-Charny, T. Wamorkar, B. Wang, A. Wisecarver, D. Wood

Northwestern University, Evanston, USA

S. Bhattacharya, J. Bueghly, Z. Chen, A. Gilbert, T. Gunter, K.A. Hahn, N. Odell, M.H. Schmitt, K. Sung, M. Velasco

University of Notre Dame, Notre Dame, USA

R. Bucci, N. Dev, R. Goldouzian, M. Hildreth, K. Hurtado Anampa, C. Jessop, K. Lannon, N. Loukas, N. Marinelli, I. Mcalister, F. Meng, K. Mohrman, Y. Musienko⁴⁷, R. Ruchti, P. Siddireddy, M. Wayne, A. Wightman, M. Wolf, L. Zygala

The Ohio State University, Columbus, USA

J. Alimena, B. Bylsma, B. Cardwell, L.S. Durkin, B. Francis, C. Hill, A. Lefeld, B.L. Winer, B.R. Yates

Princeton University, Princeton, USA

F.M. Addesa, B. Bonham, P. Das, G. Dezoort, P. Elmer, A. Frankenthal, B. Greenberg, N. Haubrich, S. Higginbotham, A. Kalogeropoulos, G. Kopp, S. Kwan, D. Lange, M.T. Lucchini, D. Marlow, K. Mei, I. Ojalvo, J. Olsen, C. Palmer, D. Stickland, C. Tully

University of Puerto Rico, Mayaguez, USA

S. Malik, S. Norberg

Purdue University, West Lafayette, USA

A.S. Bakshi, V.E. Barnes, R. Chawla, S. Das, L. Gutay, M. Jones, A.W. Jung, S. Karmarkar, M. Liu, G. Negro, N. Neumeister, C.C. Peng, S. Piperov, A. Purohit, J.F. Schulte, M. Stojanovic¹⁵, J. Thieman, F. Wang, R. Xiao, W. Xie

Purdue University Northwest, Hammond, USA

J. Dolen, N. Parashar

Rice University, Houston, USA

A. Baty, S. Dildick, K.M. Ecklund, S. Freed, F.J.M. Geurts, A. Kumar, W. Li, B.P. Padley, R. Redjimi, J. Roberts[†], W. Shi, A.G. Stahl Leitton

University of Rochester, Rochester, USA

A. Bodek, P. de Barbaro, R. Demina, J.L. Dulemba, C. Fallon, T. Ferbel, M. Galanti, A. Garcia-Bellido, O. Hindrichs, A. Khukhunaishvili, E. Ranken, R. Taus

Rutgers, The State University of New Jersey, Piscataway, USA

B. Chiarito, J.P. Chou, A. Gandrakota, Y. Gershtein, E. Halkiadakis, A. Hart, M. Heindl, E. Hughes, S. Kaplan, O. Karacheban²³, I. Laflotte, A. Lath, R. Montalvo, K. Nash, M. Osherson, S. Salur, S. Schnetzer, S. Somalwar, R. Stone, S.A. Thayil, S. Thomas, H. Wang

University of Tennessee, Knoxville, USA

H. Acharya, A.G. Delannoy, S. Spanier

Texas A&M University, College Station, USA

O. Bouhali⁹¹, M. Dalchenko, A. Delgado, R. Eusebi, J. Gilmore, T. Huang, T. Kamon⁹², H. Kim, S. Luo, S. Malhotra, R. Mueller, D. Overton, D. Rathjens, A. Safonov

Texas Tech University, Lubbock, USA

N. Akchurin, J. Damgov, V. Hegde, S. Kunori, K. Lamichhane, S.W. Lee, T. Mengke, S. Muthumuni, T. Peltola, S. Undleeb, I. Volobouev, Z. Wang, A. Whitbeck

Vanderbilt University, Nashville, USA

E. Appelt, S. Greene, A. Gurrola, W. Johns, C. Maguire, A. Melo, H. Ni, K. Padeken, F. Romeo, P. Sheldon, S. Tuo, J. Velkovska

University of Virginia, Charlottesville, USA

M.W. Arenton, B. Cox, G. Cummings, J. Hakala, R. Hirosky, M. Joyce, A. Ledovskoy, A. Li, C. Neu, B. Tannenwald, E. Wolfe

Wayne State University, Detroit, USA

P.E. Karchin, N. Poudyal, P. Thapa

University of Wisconsin - Madison, Madison, WI, USA

K. Black, T. Bose, J. Buchanan, C. Caillol, S. Dasu, I. De Bruyn, P. Everaerts, C. Galloni, H. He, M. Herndon, A. Hervé, U. Hussain, A. Lanaro, A. Loeliger, R. Loveless, J. Madhusudanan Sreekala, A. Mallampalli, A. Mohammadi, D. Pinna, A. Savin, V. Shang, V. Sharma, W.H. Smith, D. Teague, S. Trembath-reichert, W. Vetens

†: Deceased

1: Also at Vienna University of Technology, Vienna, Austria

2: Also at Institute of Basic and Applied Sciences, Faculty of Engineering, Arab Academy for Science, Technology and Maritime Transport, Alexandria, Egypt, Alexandria, Egypt

3: Also at Université Libre de Bruxelles, Bruxelles, Belgium

4: Also at IRFU, CEA, Université Paris-Saclay, Gif-sur-Yvette, France

- 5: Also at Universidade Estadual de Campinas, Campinas, Brazil
- 6: Also at Federal University of Rio Grande do Sul, Porto Alegre, Brazil
- 7: Also at UFMS, Nova Andradina, Brazil
- 8: Also at Nanjing Normal University Department of Physics, Nanjing, China
- 9: Now at The University of Iowa, Iowa City, USA
- 10: Also at University of Chinese Academy of Sciences, Beijing, China
- 11: Also at Institute for Theoretical and Experimental Physics named by A.I. Alikhanov of NRC 'Kurchatov Institute', Moscow, Russia
- 12: Also at Joint Institute for Nuclear Research, Dubna, Russia
- 13: Also at Ain Shams University, Cairo, Egypt
- 14: Now at British University in Egypt, Cairo, Egypt
- 15: Also at Purdue University, West Lafayette, USA
- 16: Also at Université de Haute Alsace, Mulhouse, France
- 17: Also at Ilia State University, Tbilisi, Georgia
- 18: Also at Erzincan Binali Yildirim University, Erzincan, Turkey
- 19: Also at CERN, European Organization for Nuclear Research, Geneva, Switzerland
- 20: Also at RWTH Aachen University, III. Physikalisches Institut A, Aachen, Germany
- 21: Also at University of Hamburg, Hamburg, Germany
- 22: Also at Department of Physics, Isfahan University of Technology, Isfahan, Iran, Isfahan, Iran
- 23: Also at Brandenburg University of Technology, Cottbus, Germany
- 24: Also at Skobeltsyn Institute of Nuclear Physics, Lomonosov Moscow State University, Moscow, Russia
- 25: Also at Physics Department, Faculty of Science, Assiut University, Assiut, Egypt
- 26: Also at Eszterhazy Karoly University, Karoly Robert Campus, Gyongyos, Hungary
- 27: Also at Institute of Physics, University of Debrecen, Debrecen, Hungary, Debrecen, Hungary
- 28: Also at Institute of Nuclear Research ATOMKI, Debrecen, Hungary
- 29: Also at MTA-ELTE Lendület CMS Particle and Nuclear Physics Group, Eötvös Loránd University, Budapest, Hungary, Budapest, Hungary
- 30: Also at Wigner Research Centre for Physics, Budapest, Hungary
- 31: Also at IIT Bhubaneswar, Bhubaneswar, India, Bhubaneswar, India
- 32: Also at Institute of Physics, Bhubaneswar, India
- 33: Also at G.H.G. Khalsa College, Punjab, India
- 34: Also at Shoolini University, Solan, India
- 35: Also at University of Hyderabad, Hyderabad, India
- 36: Also at University of Visva-Bharati, Santiniketan, India
- 37: Also at Indian Institute of Technology (IIT), Mumbai, India
- 38: Also at Deutsches Elektronen-Synchrotron, Hamburg, Germany
- 39: Also at Sharif University of Technology, Tehran, Iran
- 40: Also at Department of Physics, University of Science and Technology of Mazandaran, Behshahr, Iran
- 41: Now at INFN Sezione di Bari ^a, Università di Bari ^b, Politecnico di Bari ^c, Bari, Italy
- 42: Also at Italian National Agency for New Technologies, Energy and Sustainable Economic Development, Bologna, Italy
- 43: Also at Centro Siciliano di Fisica Nucleare e di Struttura Della Materia, Catania, Italy
- 44: Also at Università di Napoli 'Federico II', NAPOLI, Italy
- 45: Also at Riga Technical University, Riga, Latvia, Riga, Latvia
- 46: Also at Consejo Nacional de Ciencia y Tecnología, Mexico City, Mexico

-
- 47: Also at Institute for Nuclear Research, Moscow, Russia
48: Now at National Research Nuclear University 'Moscow Engineering Physics Institute' (MEPhI), Moscow, Russia
49: Also at St. Petersburg State Polytechnical University, St. Petersburg, Russia
50: Also at University of Florida, Gainesville, USA
51: Also at Imperial College, London, United Kingdom
52: Also at Moscow Institute of Physics and Technology, Moscow, Russia, Moscow, Russia
53: Also at California Institute of Technology, Pasadena, USA
54: Also at Budker Institute of Nuclear Physics, Novosibirsk, Russia
55: Also at Faculty of Physics, University of Belgrade, Belgrade, Serbia
56: Also at Trincomalee Campus, Eastern University, Sri Lanka, Nilaveli, Sri Lanka
57: Also at INFN Sezione di Pavia ^a, Università di Pavia ^b, Pavia, Italy, Pavia, Italy
58: Also at National and Kapodistrian University of Athens, Athens, Greece
59: Also at Universität Zürich, Zurich, Switzerland
60: Also at Ecole Polytechnique Fédérale Lausanne, Lausanne, Switzerland
61: Also at Stefan Meyer Institute for Subatomic Physics, Vienna, Austria, Vienna, Austria
62: Also at Laboratoire d'Annecy-le-Vieux de Physique des Particules, IN2P3-CNRS, Annecy-le-Vieux, France
63: Also at Şırnak University, Sirnak, Turkey
64: Also at Department of Physics, Tsinghua University, Beijing, China, Beijing, China
65: Also at Near East University, Research Center of Experimental Health Science, Nicosia, Turkey
66: Also at Beykent University, Istanbul, Turkey, Istanbul, Turkey
67: Also at Istanbul Aydin University, Application and Research Center for Advanced Studies (App. & Res. Cent. for Advanced Studies), Istanbul, Turkey
68: Also at Mersin University, Mersin, Turkey
69: Also at Piri Reis University, Istanbul, Turkey
70: Also at Adiyaman University, Adiyaman, Turkey
71: Also at Ozyegin University, Istanbul, Turkey
72: Also at Izmir Institute of Technology, Izmir, Turkey
73: Also at Necmettin Erbakan University, Konya, Turkey
74: Also at Bozok Universitetesi Rektörlüğü, Yozgat, Turkey, Yozgat, Turkey
75: Also at Marmara University, Istanbul, Turkey
76: Also at Milli Savunma University, Istanbul, Turkey
77: Also at Kafkas University, Kars, Turkey
78: Also at Istanbul Bilgi University, Istanbul, Turkey
79: Also at Hacettepe University, Ankara, Turkey
80: Also at Vrije Universiteit Brussel, Brussel, Belgium
81: Also at School of Physics and Astronomy, University of Southampton, Southampton, United Kingdom
82: Also at IPPP Durham University, Durham, United Kingdom
83: Also at Monash University, Faculty of Science, Clayton, Australia
84: Also at Bethel University, St. Paul, Minneapolis, USA, St. Paul, USA
85: Also at Karamanoğlu Mehmetbey University, Karaman, Turkey
86: Also at Bingol University, Bingol, Turkey
87: Also at Georgian Technical University, Tbilisi, Georgia
88: Also at Sinop University, Sinop, Turkey
89: Also at Mimar Sinan University, Istanbul, Istanbul, Turkey
90: Also at Erciyes University, KAYSERI, Turkey

91: Also at Texas A&M University at Qatar, Doha, Qatar

92: Also at Kyungpook National University, Daegu, Korea, Daegu, Korea